International Geology Review

ISSN: 0020-6814 (Print) 1938-2839 (Online) Journal homepage: http://www.tandfonline.com/loi/tigr20

Geochronology and Stable Isotope Geochemistry of UHP Metamorphic Rocks at Taohang in the Sulu Orogen, East-Central China

Bing Gong , Yong-Fei Zheng , Yuan-Bao Wu , Zi-Fu Zhao , Tianshan Gao , Jun Tang , Ren-Xu Chen , Bin Fu & Xiaoming Liu

To cite this article: Bing Gong , Yong-Fei Zheng , Yuan-Bao Wu , Zi-Fu Zhao , Tianshan Gao , Jun Tang , Ren-Xu Chen , Bin Fu & Xiaoming Liu (2007) Geochronology and Stable Isotope Geochemistry of UHP Metamorphic Rocks at Taohang in the Sulu Orogen, East-Central China, International Geology Review, 49:3, 259-286, DOI: 10.2747/0020-6814.49.3.259

To link to this article: http://dx.doi.org/10.2747/0020-6814.49.3.259

Published online: 06 Aug 2010.

International Geology Review, Vol. 49, 2007, p. 259–286.

Geochronology and Stable Isotope Geochemistry of UHP Metamorphic Rocks at Taohang in the Sulu Orogen, East-Central China

BING GONG, YONG-FEI ZHENG,[1] YUAN-BAO WU, ZI-FU ZHAO,
TIANSHAN GAO, JUN TANG, REN-XU CHEN, BIN FU,

CAS Key Laboratory of Crust-Mantle Materials and Environments, School of Earth and Space Science, University of Science and Technology of China, Hefei 230026, China

AND XIAOMING LIU

MOE Key Laboratory of Continental Dynamics, Department of Geology, Northwest University, Xi'an 710069, China

Abstract

Zircon U-Pb dating, mineral Sm-Nd isochron dating, and O and H isotope analyses were carried out for ultrahigh-pressure (UHP) eclogite and granitic gneiss from Taohang in the Sulu orogen. Besides heterogeneous ^{18}O depletion on an outcrop scale, mineral-pair O isotope thermometry indicates that refractory garnet and zircon attained and preserved equilibrium fractionations at about 820 to 560°C under eclogite-facies conditions. Zircons from the UHP metamorphic rocks have low $\delta^{18}O$ values of –1.3 to 4.2‰, variably lower than $\delta^{18}O$ values of 5.3 ± 0.3‰ for normal mantle zircons. U-Pb discordia dating of ^{18}O-depleted zircons yields a protolith age of 770 ± 23 Ma and a metamorphic age of 214 ± 9 Ma. Therefore, the ^{18}O-depleted zircons crystallized from a mid-Neoproterozoic low-^{18}O magma whose precursor experienced high-T meteoric-hydrothermal alteration prior to melting in an active rifting zone. Both H isotope composition and H_2O concentration were measured by the TCEA-MS online technique. The results show δD values of –121 to –58‰ for nominally anhydrous minerals and –101 to –62‰ for hydroxyl-bearing minerals, consistent with incorporation of meteoric water into protoliths of UHP meta-igneous rocks by high-T alteration and remelting. Hundreds to thousands of ppm H_2O were detected in the forms of both molecular water and structural hydroxyl to be present in the nominally anhydrous minerals, providing an important budget of water content (besides hydrous minerals) in deeply subducted continental crust.

A Gt-Wr-Pl Sm-Nd isochron age of 214 ± 10 Ma was obtained, in agreement with the zircon U-Pb age and corresponding to the state of O isotope equilibrium between the isochron minerals. Thus both ages are interpreted to represent the time of high-pressure eclogite-facies recrystallization during the initial exhumation. A fluid-present process for zircon overgrowth and Nd-O isotopic reequilibration is evident for this episode of retrogression. On the other hand, a Gt-Kfs Sm-Nd isochron age of 164 ± 11 Ma was obtained, corresponding to the state of O isotope disequilibrium between garnet and K-feldspar. This age postdates the Triassic collision orogeny, and thus has no relevance to the processes of both continental subduction and exhumation, suggesting limited fluid activity in the post-collisional stage. Therefore, the state of O isotope equilibrium or disequilibrium between coexisting minerals in high-grade metamorphic rocks provides a direct test for the validity of the mineral Sm-Nd chronometer in either case.

Introduction

SINCE DISCOVERY OF coesite and micro-diamond inclusions in eclogites from the Dabie-Sulu orogenic belt in east-central China (Okay et al., 1989; Wang et al., 1989; Xu et al., 1992), many studies have concentrated on the stable isotope geochemistry of ultrahigh-pressure (UHP) metamorphic rocks, with particular interest in chemical geodynamics and the fluid regime (Zheng et al., 2003a, and references therein). The presence of anomalously low $\delta^{18}O$ values of –11 to –2‰ in the UHP eclogites and gneisses indicates exchange of meteoric water with their protoliths before subduction (Yui et al., 1995, 1997; Zheng et al., 1996, 1998, 1999; Baker et al., 1997; Rumble and Yui, 1998; Fu et al., 1999). Very

[1]Corresponding author; email: yfzheng@ustc.edu.cn

limited fluid mobility is demonstrated to have occurred during UHP metamorphism by the Triassic subducton of continental crust to mantle depths (Zheng et al., 2003a). As argued by Zheng et al. (2003), continent-continent collision is not only characterized in geodynamic processes by fast subduction and fast exhumation of cold slabs with short-lived residence for UHP metamorphism at mantle depths, but also its fluid regime is attributed to internal redistribution of preexisting water that attests to significant activity during the exhumation with major derivation from decompression exsolution of hydroxyl in nominally anhydrous minerals.

Zircon U-Pb geochronology has been successfully used to define the timing of UHP metamorphism in the Dabie-Sulu orogenic belt (e.g., Ames et al., 1996; Hacker et al., 1998; Ayers et al., 2002; Li et al., 2004; Liu and Xu, 2004; Liu et al., 2004a, 2004b; Wan et al., 2005; Zheng et al., 2005a). The UHP metamorphic event has been dated for different types of UHP rocks at different outcrops, ranging from U-Pb ages of 240 ± 1 Ma (Hacker et al., 1998, 2000) to the mineral Sm-Nd isochron ages of 236 ± 4 Ma (Li et al. 2004) to 226 ± 3 (Li et al., 2000). A more tight constraint is placed by SHRIMP U-Pb ages of 234 ± 4 to 227 ± 2 Ma for coesite-bearing domains of zircon from UHP gneisses (Liu and Xu et al., 2004; Liu et al., 2004a, 2004b). These age differences may indicate that the termination timing of peak UHP metamorphism may be different for the different slices of deeply subducted slab. Nevertheless, overall period of UHP metamorphism is constrained at 240 to 225 Ma (Li et al., 2004; Wan et al., 2005), with a timescale of ~ 245–240 Ma to 210–205 Ma for both subduction and exhumation in the orogenic HP-UHP-HP regimes. Furthermore, U-Pb dating for ^{18}O-depleted zircons from different metamorphic grades of metabasite and metagranite in the Dabie-Sulu orogenic belt yields Neoproterozoic ages of 758 ± 15 Ma for UHP meta-igneous protoliths (Zheng et al., 2004). A combined study of zircon U-Pb dating and Hf-O isotope analyses demonstrates new addition of depleted mantle material to continental crust by rift magmatism in the northern margin of the South China Block, with coeval crust-mantle interaction in the mid-Neoproterozoic tectonic rifting zone (Zheng et al., 2006). Thus the low $\delta^{18}O$ zircons are the product of high-T meteoric-hydrothermal alteration or crystallization from low $\delta^{18}O$ magmas whose source experienced meteoric-hydrothermal alteration before remelting in an active rifting zone (Rumble et al., 2002; Zheng et al., 2004).

In Sm-Nd and Rb-Sr isotopic geochronology of metamorphic rocks, on the other hand, an important question is whether isotopic systems of mineral isochrons achieved isotopic equilibrium during a given metamorphic event and preserved the equilibrium afterward. Because rates of Sm-Nd, Sr, and O diffusion in metamorphic minerals are comparable in many cases, the state of O isotope equilibrium between the minerals can provide a test for the validity of mineral Sm-Nd and Rb-Sr isochrons (Zheng et al., 2002, 2003b, 2003c; Xie et al., 2004). This paper presents a combined study of zircon U-Pb and mineral Sm-Nd ages, and O and H isotopes in UHP eclogite and granitic gneiss from Taohang in the Sulu orogen. The results not only place constraints on genesis of the low $\delta^{18}O$ zircons and origin of the retrograde fluid, but also explore the validity of O isotope constraints on the Sm-Nd chronometer under different metamorphic conditions.

Geological Setting and Samples

UHP metamorphic rocks in the Dabie-Sulu orogenic belt record Triassic continental collision between the North China Block and the South China Block (e.g., Cong, 1996; Liou and Zhang, 1996; Zheng et al., 2003a). According to field occurrence and country-rock association, three types of eclogite have generally been categoried in the Dabie-Sulu orogenic belt: (1) G-type, gneiss-hosted enclaves or layers; (2) M-type, interlayers with—or enclaves within—marble or metasilicates of sedimentary protolith (including jadeite quartzite); and (3) P-type, either members of layered mafic-ultramafic intrusions or simply in association with ultramafic rocks (peridotite or pyroxenite).

Four metamorphic stages have been recognized for high-grade units in the Dabie-Sulu orogenic belt (Ernst and Liou, 1999; Zheng et al., 2003a; Li et al., 2004): (1) peak UHP coesite/diamond eclogite-facies, recorded by the occurrence of coesite and diamond, with metamorphic temperatures of about 800 to 700°C at >2.8 GPa; (2) high-pressure (HP) quartz eclogite-facies recrystallization, represented by the coexistence of garnet and omphacite with quartz instead of coesite, with metamorphic conditions of about 750 to 600°C and 2.4 to 1.2 GPa; (3) HP granulite-facies overprinting, represented by the occurrence of orthopyroxene or plagioclase, with metamorphic conditions of about 850 to 750°C and

2.0 to 1.0 GPa; and (4) amphibolite-facies retrogression, indicated by the occurrence of various symplectites such as amphibole + sodic plagioclase and the disappearance of omphacite from eclogite, with P-T conditions of about 600 to 450°C and 1.0 to 0.6 GPa. The zones of different metamorphic grades heterogeneously crop out along the orogenic belt, which is generally bounded by blueschist-facies zones in the south but greenschist-facies zones in the north (Zheng et al., 2005b). HP quartz eclogite-facies rocks do not exist as an independent unit, but occur as a result of retrograde HP recrystallization that overprinted the UHP eclogite-facies rocks during the initial exhumation (Ernst and Liou, 1999; Zheng et al., 2003a). HP granulite-facies rocks do occur as independent units where amphibolite-facies retrogression is absent (Cong, 1996; Zheng et al., 2001).

This study deals with UHP eclogite and granitic gneiss from Taohang in the northwestern margin of the Sulu orogen (Fig. 1B). Taohang is a small village that is located about 5 km south of the Wulian-Yantai fault (Fig. 1A). The metamorphic unit consists mainly of garnet-bearing kyanite-phengite quartzite, garnet-biotite gneiss, amphibole-bearing gneiss, garnet pyroxenite, and diopside tremolite-bearing marble. Coesite pseudomorphs are present in zoisite from the eclogite (Yao et al., 2000). Also, coesite and omphacite inclusions as minute inclusions occur in zircon from a granitic orthogneiss at this locality (Ye et al., 2000). These demonstrate that both mafic and felsic metamorphic rocks experienced the UHP eclogite-facies metamorphism. A transition from eclogite-facies to granulite-facies paragenesis (Omp + Pl + Qz + Gt) occurs in the coesite-bearing eclogite (Yao et al., 2000). This transition postdated the peak UHP eclogite-facies metamorphism but predated amphibolite-facies overprinting. Such a paragenesis reequilibrated at 1.7 GPa and 820°C (Yao et al., 2000), suggesting that the granulite-facies metamorphism had activated the retrograde recrystallization at a deep crustal level. On the other hand, amphibolite-facies retrogression was identified by Ye et al. (2000) from petrology of the granitic gneiss. It appears that heterogeneous overprinting occurred in the Taohang eclogite and granitic gneiss at either high or moderate temperatures.

The eclogite and granitic gneiss samples used in this study were collected in the western gulley in Taohang mountain (Fig. 1A). The eclogite consists of garnet + omphacite ($Jd_{40}Di_{60}$) ± quartz ± zoisite ± muscovite ± zircon ± rutile. The granitic gneiss consists of quartz + plagioclase (An_{30}) + K-feldspar + garnet ± muscovite ± epidote ± biotite ± titanite ± zircon ± magnetite. Mineral abbreviations used in this paper are listed in Table 1.

Both eclogite and granitic gneiss at Taohang were dated by the SHRIMP zircon U-Pb method (Zheng et al., 2004). The results from the eclogite gave two SHRIMP $^{206}Pb/^{238}U$ spot-ages of 777 ± 9 Ma for igneous cores, with Th/U ratios of 0.74 to 0.28 for the eclogite. Although a Triassic age was not acquired from the SHRIMP data, significant Pb loss due to metamorphism is evident from the discordant distribution of U-Pb data below the concordia curve toward the Triassic age. For the granitic gneiss, the SHRIMP data only yielded a $^{206}Pb/^{238}U$ spot-age of 771 ± 9 Ma with a Th/U ratio of 0.81, and a Triassic $^{206}Pb/^{238}U$ spot-age of 227 ± 3 Ma with a low Th/U ratio of 0.18. It appears that the Taohang eclogite and granitic gneiss represent Middle Neoproterozoic protoliths with mafic and felsic compositions, respectively. They experienced Triassic UHP metamorphism during collision between the South China Block and the North China Block.

Analytical Methods

Minerals were separated for isotopic analyses. After crushing, a shaking bed was used to separate heavy minerals, followed by magnetic separation using a magnetic separator, and then purification by hand picking under the binocular microscope. All mineral separates used for O and H isotope analyses were of 40 to 60 μm grain size.

Oxygen isotope analysis was accomplished for mineral separates by the laser fluorination techniques at the University of Science and Technology of China in Hefei. A 25 W CO_2 laser MIR-10 was used: its emission wavelength is 10.6 μm, which lies in the infrared domain, and can thus be well absorbed by O-bearing compounds; its power can be adjusted in the range of 0 to 100%, which is very important during sample analysis; the diameter of the laser beam can be adjusted from 100 to 1820 μm. Minerals weighing about 1.5 to 2.0 mg were reacted with BrF_5 under vacuum. Obtained O_2 was directly transferred to a mass spectrometer for O isotope analysis. $^{18}O/^{16}O$ ratios were measured in a Delta+ mass spectrometer and reported in the $\delta^{18}O$ notation relative to the VSMOW standard. A number of replicate analyses give a reproducibility of better than ±0.1‰ (Zheng et al., 2002). Three

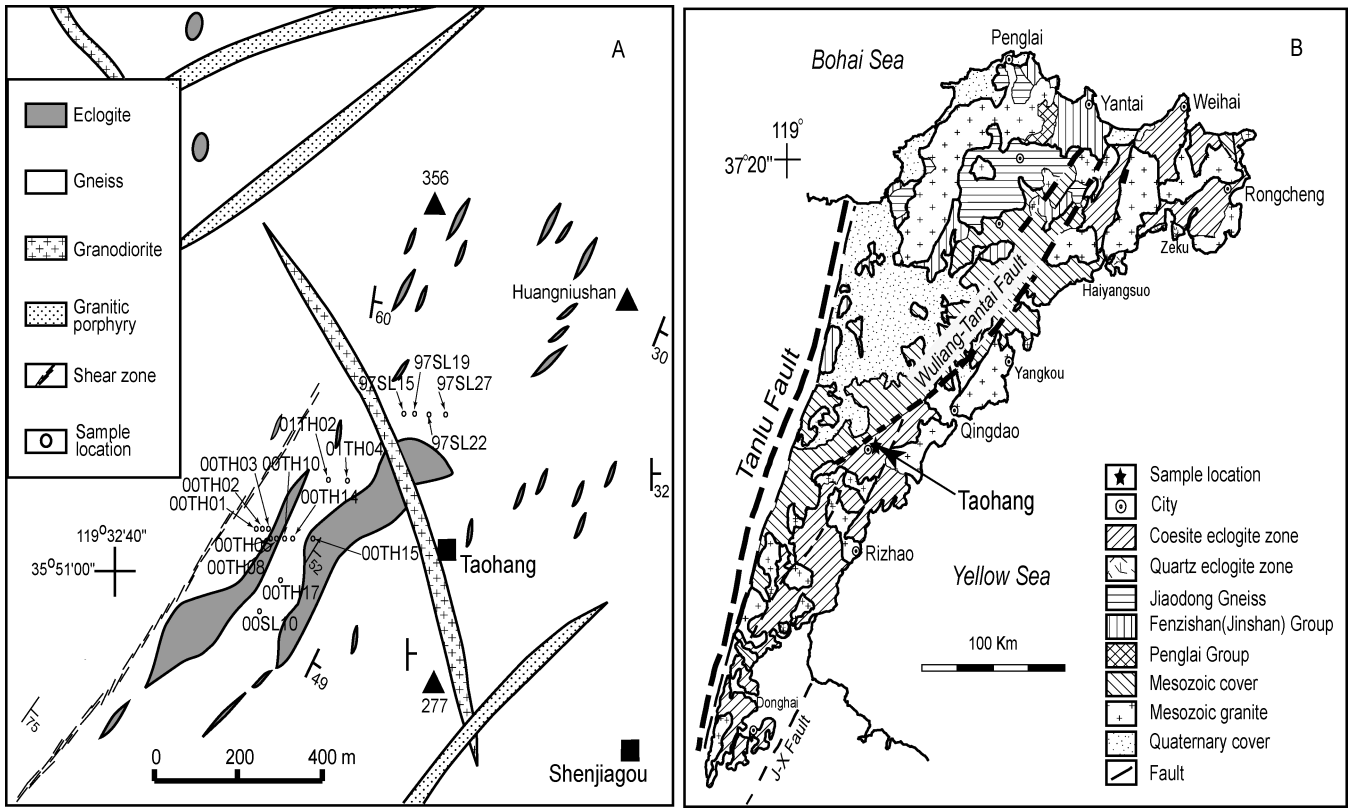

FIG. 1. Sketch map of geology at Taohang within the framework of the Sulu orogen. Sample numbers denote sample localities. A. Sketch of geological map at Taohang. B. Index map of the Sulu orogen showing the position of Taohang.

TABLE 1. Oxygen Isotope Composition and Estimated Temperatures of UHP Metamorphic Rocks from Taohang, Sulu Orogen

Sample number	Minerals	$\delta^{18}O$, ‰	Mineral pairs[1]	$\Delta^{18}O$, ‰	T, °C
		Granitic gneiss			
00TH01	Qz	5.38			
	Kfs	2.66	Qz-Kfs	2.72	270
	Pl	2.03	Qz-Pl	3.35	260
	Mus	1.84	Qz-Mus	3.54	440
	Gt	2.57	Qz-Gt	2.81	800
	Ep	2.65	Qz-Ep	2.73	610
	Mt	−3.77	Qz-Mt	9.14	460
00TH02	Qz	5.58			
	Kfs	2.32	Qz-Kfs	3.27	200
	Pl	2.27	Qz-Pl	3.32	260
	Mus	2.66	Qz-Mus	2.93	530
	Gt	2.89	Qz-Gt	2.70	820
	Mt	−3.42	Qz-Mt	9.00	470
00TH03	Qz	4.61			
	Pl	0.65	Qz-Pl	3.97	Dis
	Mus	1.69	Qz-Mus	2.93	530
	Gt	1.77	Qz-Gt	2.84	800
	Zr	1.70	Qz-Zr	2.91	775
	Mt	−2.85	Qz-Mt	7.46	550
00TH10	Qz	5.29			
	Pl	2.74	Qz-Pl	2.56	370
	Kfs	2.62	Qz-Kfs	2.67	275
	Mus	2.57	Qz-Mus	2.72	570
	Gt	2.47	Qz-Gt	2.83	800
	Ep	2.54	Qz-Ep	2.75	605
	Tn	1.95	Qz-Tt	3.35	675
	Mt	−2.80	Qz-Mt	8.09	515
00TH14	Qz	6.23			
	Gt(dark)	2.03	Qz-Gt	4.18	590
	Gt(light)	2.22	Qz-Gt	3.99	615
00TH17	Qz	1.96			
	Kfs	0.46	Qz-Kfs	1.54	515
	Pl	0.07	Qz-Pl	1.89	510
	Zr	−1.30	Qz-Zr	3.30	705
	Mt	−4.00	Qz-Mt	5.96	670

Table continues

TABLE 1. *Continued*

Sample number	Minerals	$\delta^{18}O$, ‰	Mineral pairs[1]	$\Delta^{18}O$, ‰	T, °C
		Granitic gneiss			
97SL15	Qz	6.92			
	Kfs	2.17	Qz-Kfs	4.75	Dis[2]
	Pl	1.70	Qz-Pl	5.23	Dis
	Mus	2.59	Qz-Mus	4.33	355
	Gt	3.99	Qz-Gt	2.94	780
	Zr	4.18	Qz-Zr	2.75	810
	Tn	3.46	Qz-Tt	3.47	685
	Mt	–3.05	Qz-Mt	9.97	430
97SL19	Qz	5.94			
	Kfs	1.90	Qz-Kfs	4.05	Dis
	Mus	2.46	Qz-Mus	3.48	450
	Gt	1.52	Qz-Gt	4.42	560
97SL22	Qz	5.29			
	Kfs	0.08	Qz-Kfs	5.21	Dis
	Pl	0.20	Qz-Pl	5.09	Dis
	Mus	1.53	Qz-Mus	3.76	415
	Bi	–3.37	Qz-Bi	8.66	Dis
	Ep	1.60	Qz-Ep	3.69	460
	Ep[3]	1.26	Qz-Ep	4.04	415
97SL27	Qz	6.92			
	Kfs	2.17	Qz-Kfs	4.75	Dis
	Pl	1.70	Qz-Pl	5.23	Dis
	Mus	2.59	Qz-Mus	4.33	355
	Gt	3.99	Qz-Gt	2.94	780
	Tn	3.46	Qz-Tt	3.47	660
	Mt	–3.05	Qz-Mt	9.97	425
01TH02	Qz	5.88			
	Kfs	0.95	Qz-Kfs	4.93	Dis
	Pl	0.73	Qz-Pl	5.15	Dis
	Mus	4.04	Qz-Mus	1.84	785
	Gt	2.30	Qz-Gt	3.58	670
01TH04	Qz	6.13			
	Kfs	3.98	Qz-Kfs	2.15	355
	Pl	3.75	Qz-Pl	2.38	405
	Mus	3.19	Qz-Mus	2.94	530
	Bi	1.52	Qz-Bi	4.61	495
	Gt	2.66	Qz-Gt	3.47	685

Table continues

TABLE 1. *Continued*

Sample number	Minerals	$\delta^{18}O$, ‰	Mineral pairs[1]	$\Delta^{18}O$, ‰	T, °C
		Granitic gneiss			
00SL10	Qz	6.02			
	Kfs	3.71	Qz-Kfs	2.31	325
	Pl	3.50	Qz-Pl	2.52	380
	Gt	2.54	Qz-Gt	3.48	685
	Tn	1.64	Qz-Tt	4.38	495
	Bi	0.95	Qz-Bi	5.07	450
	Ep	2.60	Qz-Ep	3.42	535
	Mt	−3.23	Qz-Mt	9.25	455
		Eclogite			
00TH06	Qz	5.43			
	Mus	2.40	Qz-Mus	3.03	515
	Omp	2.17	Qz-Omp	3.26	495
	Gt	1.10	Mus-Gt	1.30	700
	Rt	−2.27	Mus-Rt	4.67	380
00TH08	Mus	2.98			
	Gt	1.66	Mus-Gt	1.32	650
	Zr	1.78	Mus-Zr	1.20	700
	Rt	−1.47	Mus-Rt	4.45	400
00TH15	Mus	1.11			
	Omp	0.85			
	Gt	−0.05	Mus-Gt	1.16	750
	Rt	−3.11	Mus-Rt	4.22	450

[1]Mineral abbreviation: Qz = quartz; Kfs = K-feldspar; Pl (An 30) = plagioclase; Mus = muscovite; Tn = titanite; Ep = epidote; Omp ($Jd_{40}Di_{60}$) = omphacite; Gt = garnet; Zr = zircon; Rt = rutile; Mt = magnetite.
[2]T was calculated by using theoretical calculations of Zheng (1991, 1993a, 1993b), and "Dis" denotes disequilibrium fractionation.
[3]Not pure.

international standards and two national standards of China were used during the laser fluorination analyses: $\delta^{18}O$ = 5.8‰ for UWG-2 garnet (Valley et al., 1995); $\delta^{18}O$ = 5.2‰ for SCO-1 olivine (Eiler et al., 1996); $\delta^{18}O$ = 10.0‰ for 91500 zircon (Zheng et al., 2004); $\delta^{18}O$ = 11.1‰ for the National Standard of China GBW04409 quartz; $\delta^{18}O$ = −1.7‰ for the National Standard of China GBW04410 quartz.

Hydrogen isotope compositions and H_2O concentrations in minerals were simultaneously analyzed by the TCEA-MS online technique at the University of Science and Technology of China in Hefei. This is an integrated procedure using a thermal conversion elemental analyzer (TCEA) and isotope-ratio mass spectrometer (MS) with continuous flow inlet system. Similar analytical procedures were described for organic and/or inorganic compounds (e.g., Begley and Scrimgeour, 1997; Hilkert et al., 1999; Eiler and Kitchen, 2001; Sharp et al., 2001; Godin et al., 2004). In our online analysis, nevertheless, the reduction furnace and gas chromatography of a Finnigan TC/EA are combined with a MAT-253 mass spectrometer via open split in Finnigan Conflo III interface. The reduction column

consists of an 18 mm diameter ceramic tube lined with a glassy carbon sleeve. A temperature of 1450°C was used for the carbon reduction in order to obtain better precision for inorganic solid samples (Sharp et al., 2001) and longer life of the reduction furnace (Burgoyne and Hayes, 1998). As a result, both molecular water and structural hydroxyl were extracted from the minerals for the simultaneous online analyses of both bulk H_2O concentration and H isotope composition. Solid samples were wrapped in solver foil capsules and dropped into the furnace using an autosampler. All inorganic solid samples were preheated at 90°C for 12 hours to eliminate adsorption water on the sample surface. Both H_2 and CO gases were produced by the reaction of H_2O and C in a He carrier gas. They were separated in the gas chromatograph (GC) and then analyzed in the mass spectrometer in the continuous flow mode. When H_2 was analyzed, GC was operated at 90°C to decrease the retention time and minimize peak broadening. When not in use, it was heated to 300°C with a low-flow He stream for cleaning. In addition to determining D/H ratios, the time-integrated intensity of sample peak was used to determine wt% or ppm wt. H_2O. The ^4He tailing was eliminated by using an electrostatic filter in MAT-253. The H_3^+ factor was calculated by the Finnigan MAT ISODAT software for the H_3^+ ion correction. Two standards were used during the H isotope analyses: $\delta D = -65.7‰$ for NBS-30 biotite, and $\delta D = -100.3‰$ for IAEA-CH-7 Polyethylene. One standard was used during the H_2O content analyses: 5 wt% H for benzoic acid ($C_7H_6O_2$). A home-standard garnet 04BXL02 was used to control both H isotope and water content analyses, which has a δD value of –93 ± 4‰ and a total H_2O content of 524 ± 28 ppm by weight. Our protocols show the routine analysis of sample sizes as small as 0.01 μl H_2O for both H isotope composition and H_2O concentration in hydrous and nominally anhydrous minerals. Thus analytical errors appear to depend on mineral water contents, with absolute reproducibilities of about ± 4‰ (1σ) for δD values and relative uncertainties of about ± 5% to ± 10% (1σ) for H_2O concentrations. In practice, the analytical errors for the δD value and the H_2O content can respectively be as low as ± 1‰ and ± 1% for hydrous minerals, but as high as ± 6‰ and ± 10% for nominally anhydrous minerals of low water contents.

Zircon cathodoluminescence (CL) imaging was made using a JXA-8800R electron microprobe at the Institute of Mineral Resources, Chinese Academy of Geological Science, Beijing. Zircon LA-ICPMS U-Pb dating was carried out at the Department of Geology, Northwest University, Xi'an. A GeoLas 200M laser-ablation system equipped with a 193 nm ArF-excimer laser was used in connection with an ELAN6100 DRC ICPMS. Helium was used as carrier gas to enhance transport efficiency of the ablated material. The detailed analytical method was described by Yuan et al. (2004). All measurements were performed using zircon 91500 as an external standard with a $^{206}Pb/^{238}U$ age of 1065.4 ± 0.6 Ma (Wiedenbeck et al., 1995). Common Pb correction was carried out by using the EXCEL program ComPbCorr#_151 (Anderson, 2002). Ages were calculated using the ISOPLOT program of Ludwig (2001).

Sm-Nd isotopic analysis was carried out by dissolving the samples in acid (HNO_3 + HF) in sealed Savillex beakers on a hot plate. Separation of Sm and Nd was performed via a routine two-column ion exchange technique (Li et al., 1988; Wang et al., 1988). Total procedural blank for Nd is 80 pg. Nd isotopic ratios were measured on a Finnigan MAT-261 mass spectrometer at the Institute of Geology in the Chinese Academy of Geological Sciences, Beijing. The Nd isotopic ratios were corrected for mass fractionation relative to $^{146}Nd/^{144}Nd = 0.7219$. La Jolla standard yielded $^{143}Nd/^{144}Nd = 0.511860 \pm 4$ (2σ). During the period of data acquisition, the Ames internal Nd standard gave $^{143}Nd/^{144}Nd$ ratios of 0.511967 ± 2 (2σ), which is equivalent to the La Jolla value of 0.511860. Sm-Nd isochron calculations were made using the ISOPLOT program (Ludwig, 2001). Analytical precisions of isotope ratio measurements are given as ±2σ standard errors, whereas the quoted errors in ages and initial isotopic ratios represent ±2σ standard deviations.

Results

Oxygen isotopes

The O isotope composition of mineral separates for the eclogite and granitic gneiss at Taohang is presented in Table 1. They all have variable mineral $\delta^{18}O$ values: quartz 2.0 to 6.9‰, feldspar 0.1 to 4.0‰, muscovite 1.7 to 4.0‰, garnet 1.5 to 4.0‰, and zircon –1.3 to 4.2‰ for the granitic gneiss; quartz 5.4‰, garnet –0.1 to 1.7‰, omphacite 0.9 to 2.2‰, muscovite 1.1 to 3.0‰, rutile –3.3 to –1.5‰, and zircon 1.8‰ for the eclogite. Obviously, most of the samples have $\delta^{18}O$ values lower than normal metamorphic rocks that show $\delta^{18}O$ values of 6 to

18‰ (Hoefs, 1997; Sharp et al., 1988), pointing to ^{18}O depletion in the UHP metamorphic rocks. Furthermore, O isotope heterogeneity is significant on an outcrop scale. Thus any O isotope exchange during the subduction, collision, and exhumation history was limited to internal redistribution within the local lithologies.

Oxygen isotope temperatures are calculated from fractionations between quartz and the other minerals and listed in Table 1, assuming preservation of isotope equilibration at the scale of sample measurement. The results show both equilibrium and disequilibrium fractionations between the minerals in the UHP metamorphic rocks (Figs. 2, 3, and 4). On one hand, refractory mineral pairs of quartz-garnet and quartz-zircon from the granitic gneiss (Fig. 2) and muscovite-garnet from the eclogite yield temperatures of 560 to 820°C (Fig. 4), reasonable for eclogite-facies metamorphic conditions. The maximum O isotope temperatures are consistent with the petrological temperatures for granulite-facies overprinting (Yao et al., 2000), suggesting attainment and preservation of high-T O isotope equilibrium during exhumation. The preservation of high-T O isotope equilibrium also confirms the previous conclusion that the Dabie-Sulu UHP metamorphic rocks acquired their low $\delta^{18}O$ values by interaction with ^{18}O-depleted meteoric water before continental subduction

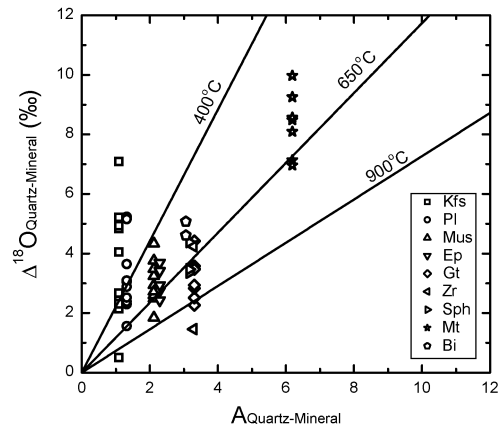

FIG. 2. Isotherm plot for O isotope fractionations between quartz and other minerals from granitic gneisses at Taohang, Sulu orogen. Data points not bracketed by 400 to 800°C isotherms are considered as disequilibrium. Fractionation curves are after Zheng (1991, 1993a, 1993b).

(Rumble and Yui, 1998; Rumble et al., 2002, 2003; Zheng et al., 1998, 1999, 2003a, 2004).

On the other hand, quartz-feldspar pairs from the granitic gneiss give either low temperatures of 200 to 515°C or too great fractionations to be at equilibrium, even if a very slow cooling is assumed (Table 1); muscovite-rutile pairs from the eclogite yield

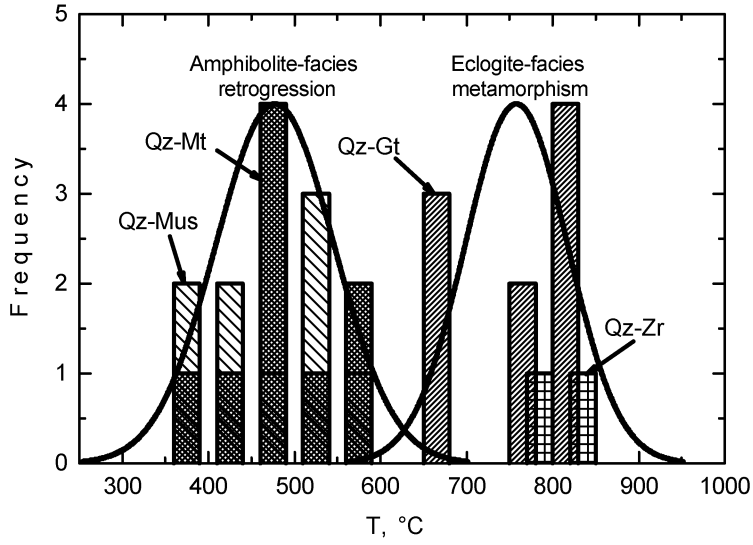

FIG. 3. Histogram for O isotopic temperatures between quartz and other minerals from granitic gneisses at Taohang, Sulu orogen.

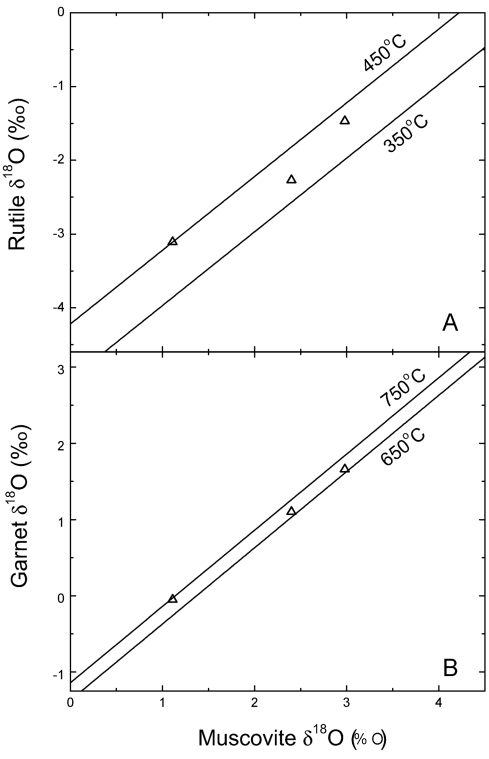

FIG. 4. $\delta^{18}O$–$\delta^{18}O$ plot between muscovite + garnet and muscovite + rutile from eclogites at Taohang, Sulu orogen.

isotopic temperatures of 380 to 450°C (Fig. 4A). These are significantly lower than the temperatures of eclogite-facies metamorphism, suggesting the effect of retrograde isotope exchange at lower temperatures than amphibolite-facies conditions. Some of the quartz-feldspar pairs from the granitic gneiss display O isotope disequilibrium due to significantly low $\delta^{18}O$ values for feldspars, indicating interaction between feldspar and low $\delta^{18}O$ fluid at moderate to high temperatures.

Hydrogen isotopes and H_2O concentrations

The H isotope composition and H_2O concentration of mineral separates for the eclogite and granitic gneiss at Taohang is listed in Table 2 and illustrated in Figure 5. Hydrous minerals from the granitic gneiss show δD values of –101 to –90‰ for muscovite and –62‰ for epidote, and muscovite from the eclogite has δD values of –94 to –77‰. Nominally anhydrous minerals from the eclogite have δD values of –119 to –99‰ for omphacite, –106 to –80‰ for garnet, –121 to –97‰ for rutile, and –78‰ for quartz; those from the granitic gneiss have δD values of –73 to –68‰ for feldspars, –65 to –58‰ for quartz, –113 to –96 for magnetite, –82‰ for titanite, and –69‰ for apatite. For the eclogite, omphacite and rutile have similar δD values to each other, but both are lower than similar δD values for muscovite and garnet (Fig. 5A). For the granitic gneiss, magnetite has the lowest δD values whereas epidote and quartz have the highest δD values; muscovite and garnet exhibit similar δD values to each other like those in the eclogite; feldspars and apatite have similar δD values to each other (Fig. 5B).

Eclogite shows H_2O concentrations of 1278 to 1845 ppm in omphacite, 531 to 819 ppm in garnet, 1620 to 1764 ppm in rutile, and 294 ppm in quartz (Fig. 5A). The gneiss minerals have H_2O concentrations of 711 to 1557 ppm in feldspars, 351 to 386 ppm in quartz, 3987 to 4617 ppm in magnetite, 1017 to 1539 ppm in garnet, 4041 ppm in titanite, and 882 ppm in apatite (Fig. 5B). Significant amounts of H_2O apparently are present in these nominally anhydrous minerals. Hydroxyl-bearing minerals were also measured to have variable H_2O concentrations of 41,715 to 46,647 ppm for muscovite and 26,118 ppm for epidote. Despite the similar δD values (Fig. 5), garnet from the granitic gneiss has much higher H_2O concentrations than that in the eclogite. In contrast, quartz from the eclogite has much a much higher H_2O concentration than that in the granitic gneiss. Significant amounts of H_2O are also present in magnetite, titanite, and rutile.

It is worth noting that the TCEA-MS method extracts both molecular H_2O and structural OH from minerals for a simultaneous determination of both bulk H_2O concentration and H isotope composition. It remains to resolve how much each species of water is present in the minerals in question, and whether the two species of water have distinct δD values with respect to their origin. Stepwise heating may be a potential means of extracting the different species of water, and Fournier Transform Infrared Spectra (FTIR) analysis can be used to test whether the mineral samples after high-T heating only contain the structural OH.

Isotopic dating

LA-ICPMS U-Pb dating and CL imaging were carried out for zircons from granitic gneiss 00TH03. The results are presented in Table 3 and Figures 6 and 7. Zircons from this granitic gneiss are short to

TABLE 2. Hydrogen Isotope Composition and H_2O Concentration of Mineral Separates from UHP Metamorphic Rocks at Taohang, Sulu Orogen

Rock type	Sample no.	Mineral[1]	H, ppm	H_2O, ppm	δD, ‰
Eclogite	00TH06	Qz	294	2646	–78
		Mus	4635	41715	–77
		Omp	142	1278	–98
		Gt	59	531	–80
		Rt	196	1764	–97
Eclogite	00TH08	Mus	5060	45540	–96
Eclogite	00TH15	Mus	5051	45459	–94
		Omp	205	1845	–119
		Gt	91	819	–106
		Rt	180	1620	–121
Granitic gneiss	00TH01	Qz	54	486	–65
		Pl	79	711	–71
		Mus	5183	46647	–90
		Ep	2902	26118	–62
		Gt	171	1539	–102
		Mt	443	3987	–96
Granitic gneiss	00TH02	Gt	141	1269	–99
Granitic gneiss	00TH03	Qz	39	351	–58
		Pl	83	747	–68
		Mus	5072	45648	–98
		Mt	494	4446	–112
Granitic gneiss	97SL15	Qz	39	351	–64
		Kfs	173	1557	–73
		Pl	89	801	–73
		Mus	5009	45081	–101
		Gt	113	1017	–77
		Tn	449	4041	–82
		Mt	513	4617	–113
		Ap	98	882	–69

[1]Mineral abbreviation: Qz = quartz; Kfs = K-feldspar; Pl = plagioclase; Mus = muscovite; Tn = titanite; Ep = epidote; Omp = omphacite; Gt = garnet; Rt = rutile; Mt = magnetite; Ap = aptite.

long prismatic, colorless, and transparent under the microscope. They are subhedral, and some grains are present as fragments. All of the zircons in the CL images display core-rim structure (Fig. 6). Most of the cores show oscillatory zoning, which is typical for magmatic environments. Some cores only preserve patchy or planar zoning, which may result from solid-state recrystallization. Corrosion of oscillatory-zoned domains is visible around the cores. Very thin (always <10 μm) structureless rims of weak luminescence are present on most grains due to metamorphic overgrowth.

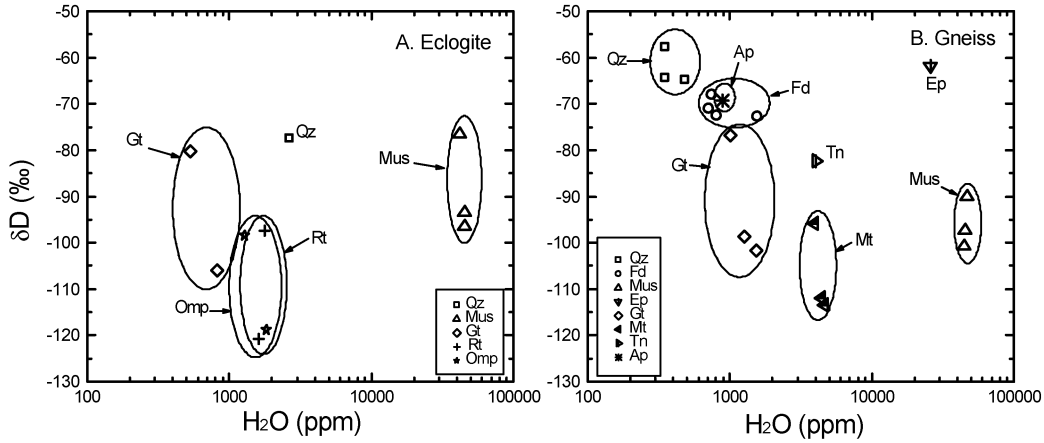

FIG. 5. Plot of H isotope composition and H_2O concentration of mineral separates from eclogite and granitic gneiss at Taohang, Sulu orogen.

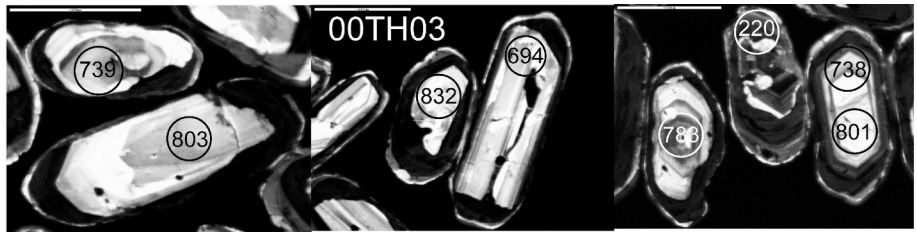

FIG. 6. CL imaging for zircons from eclogite at Taohang, Sulu orogen.

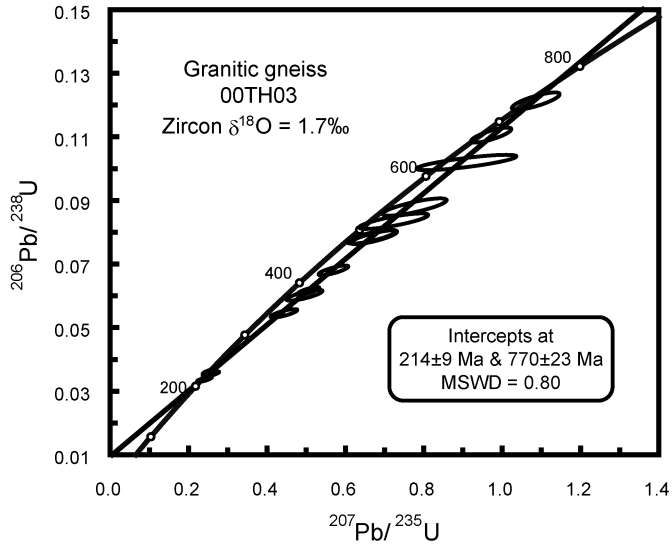

FIG. 7. Zircon U-Pb concordia diagram for granitic gneiss at Taohang, Sulu orogen.

TABLE 3. LA-ICP-MS Zircon U-Pb Isotope Data for Granitic Gneiss from Taohang, Sulu Orogen

No.	Element, ppm				Isotopic ratio										Age (Ma)					
	Th	U	Total, Pb	Th/U	$^{207}Pb/^{206}Pb$	1σ	$^{207}Pb/^{235}U$	1σ	$^{206}Pb/^{238}U$	1σ	$^{208}Pb/^{232}Th$	1σ	$^{238}U/^{232}Th$	1σ	$^{207}Pb/^{206}Pb$	1σ	$^{207}Pb/^{235}U$	1σ	$^{206}Pb/^{238}U$	1σ
1	84.5	210.1	50.76	0.40	0.06259	0.00632	0.721633	0.07197	0.08362	0.00203	0.03386	0.0009	2.47	0.02	694	201.6	552	42.4	518	12.1
2	54.0	143.9	40.37	0.38	0.06042	0.00333	0.568071	0.03109	0.06819	0.00128	0.04808	0.0013	2.64	0.03	619	100.6	457	19.4	425	7.8
3	67.0	138.9	41.86	0.48	0.06191	0.00459	0.670685	0.04887	0.07857	0.00181	0.03644	0.0012	2.06	0.02	671	151.2	521	29.7	488	10.8
4	78.2	95.9	27.69	0.82	0.05924	0.00266	0.504048	0.02267	0.06171	0.00107	0.03252	0.0007	1.22	0.01	576	88.31	414	15.0	386	6.5
5	148.4	269.0	41.91	0.55	0.05195	0.00346	0.254926	0.01679	0.03559	0.00071	0.01297	0.0004	1.8	0.02	283	132.1	231	13.4	225	4.4
6	51.6	68.2	19.13	0.76	0.06388	0.00559	0.775877	0.06662	0.08809	0.00224	0.03609	0.0011	1.31	0.01	738	175.2	583	38.1	544	13.3
7	108.2	150.3	62.77	0.72	0.06366	0.00277	0.970961	0.04236	0.11062	0.00195	0.03365	0.0007	1.38	0.01	730	80.8	689	21.0	676	11.3
8	151.4	197.5	72.45	0.77	0.06485	0.00298	1.084785	0.04974	0.12132	0.00222	0.03767	0.0008	1.3	0.01	769	92.1	746	24.0	738	12.8
9	45.8	399.9	67.86	0.11	0.05117	0.00342	0.238964	0.01577	0.03387	0.00069	0.01928	0.0023	8.67	0.09	248	144.7	218	12.9	215	4.3
10	54.5	469.1	82.24	0.12	0.04964	0.00224	0.247834	0.0112	0.03621	0.00063	0.0213	0.0017	8.54	0.09	178	101.9	225	9.1	229	3.9
11	43.6	594.2	86.99	0.07	0.05201	0.00273	0.256081	0.01202	0.03571	0.00059	0.01989	0.0015	13.54	0.14	286	115.7	232	9.9	226	3.7
12	66.6	93.0	20.67	0.72	0.05859	0.00384	0.441484	0.02854	0.05465	0.0011	0.02904	0.0008	1.39	0.01	552	117.5	371	19.4	343	6.7
13	60.5	315.9	51.65	0.19	0.05932	0.00461	0.493932	0.03768	0.06039	0.00138	0.03059	0.001	5.19	0.05	579	145.7	408	25.0	378	8.4
14	65.1	100.0	35.69	0.06	0.06450	0.0863	0.907824	0.10404	0.10208	0.00202	0.00049	0.0008	1.53	0.02	758	179	656	35	627	12
15	61.2	70.3	21.84	0.87	0.06127	0.00477	0.665273	0.05080	0.07875	0.0018	0.03596	0.0011	1.14	0.01	649	146.4	518	30.2	489	10.8
16	24.0	795.0	113.43	0.03	0.05154	0.00138	0.248793	0.00693	0.03501	0.00053	0.01163	0.0007	32.96	0.33	265	60.1	226	5.6	222	3.3

TABLE 4. Sm-Nd Isotope Composition of Minerals and Whole-Rock from Granitic Gneiss at Taohang, Sulu Orogen

Sample	Mineral	Sm, ppm	Nd, ppm	$^{147}Sm/^{144}Nd$	$^{143}Nd/^{144}Nd \pm 2\sigma$
01TH02	Whole-rock	11.7	61.24	0.1155	0.511755 ± 8
	Garnet	2.53	4.78	0.3208	0.511988 ± 10
	K-feldspar	0.78	3.57	0.1317	0.511785 ± 10
01TH04	Whole-rock	11.54	58.27	0.1198	0.511731 ± 12
	Garnet	1.25	2.42	0.3112	0.511999 ± 8
	Plagioclase	0.35	0.99	0.2154	0.511858 ± 15

As illustrated in Figure 7, U–Pb discordia dating defines an upper intercept age of 770 ± 23 Ma and a lower intercept age of 214 ± 9 Ma. The two ages are consistent with the known SHRIMP zircon U-Pb dates for the Taohang eclogite and granitic gneiss (Zheng e al., 2004). Thus they date crystallization of magmatic cores and growth of metamorphic rims (Fig. 6), reflecting the time of protolith crystallization and of the HP metamorphic overprinting stage. Mineral and whole-rock Sm-Nd isotopic data for two samples of the granitic gneiss from Taohang are listed in Table 4. The results yield a Gt-Pl-Wr isochron age of 214 ± 10 Ma for sample 01TH04 (Fig. 8A), and a Gt–Kfs isochron age of 164 ± 11 Ma for sample 01TH02 (Fig. 8B).

Discussion

The old LA-ICPMS age of 770 ± 23 Ma from this study agrees with the known SHRIMP date at 771 ± 9 Ma for the same lithology at Taohang (Zheng et al., 2004). This indicates that the protolith of the granitic gneiss at Taohang is clearly of Middle Neoproterozoic age, similar to protoliths of other UHP meta-igneous rocks in the Dabie-Sulu orogenic belt (Ames et al., 1996; Rowley et al., 1997; Hacker et al., 1998; Zheng et al., 2003a, 2004, 2005a, 2006). However, the low $\delta^{18}O$ values for the zircon and rock-forming minerals need to be interpreted together with the radiometric ages.

The consistent ages of 214 ± 9 Ma and 214 ± 10 Ma were obtained from the zircon U-Pb system and the mineral–whole rock Sm-Nd system for the granitic gneiss. These ages are somewhat lower than the SHRIMP zircon U-Pb date at 227 ± 3 Ma (Zheng et al., 2004), but in general agreement with known dates by Sm-Nd, Rb-Sr, and U-Pb methods for eclogite-facies metamorphism in the Dabie-Sulu orogenic belt (e.g., Chavagnac and Jahn, 1996; Li et al., 1999, 2000). This suggests that Sm-Nd isotope equilibrium was attained during the Triassic UHP metamorphism and preserved afterward. There is a small difference in age between 214 ± 10 Ma and 227 ± 3 Ma from the two data sets, but the larger errors of ±9–10 Ma are associated with the present dates than the previous date. This may imply that the present dates register timing of an episodic retrogression during the initial exhumation, probably at the HP eclogite-facies phase.

On the other hand, neither a metamorphic nor a magmatic event has been identified so far as occurring at about 160 to 180 Ma in this orogenic belt (Cong, 1996; Li et al., 1999; Hacker et al., 2000). The cycle of continental collision recorded in the Dabie-Sulu orogenic belt has been dated at ~245–240 Ma to 210–205 Ma for both subduction and exhumation in the HP-UHP-HP regimes (Li et al., 2004; Wan et al., 2005; Zheng et al., 2005a). Thus the Gt-Kfs isochron age of 164 ± 11 Ma remains to be interpreted along with O isotopic disequilibrium, as indicated by a negative $\Delta^{18}O$ value of –1.35‰ between garnet and K-feldspar (Table 1).

Genesis of low $\delta^{18}O$ zircons

UHP metamorphic rocks from Taohang have zircon $\delta^{18}O$ values of –1.3 to 4.2‰ (Table 1). They are lower than normal mantle zircon $\delta^{18}O$ values of 5.3 ± 0.3‰ (Valley et al., 1998), pointing to relative ^{18}O deleption. As documented by Zheng et al. (2004), the capability of preserving the O isotope

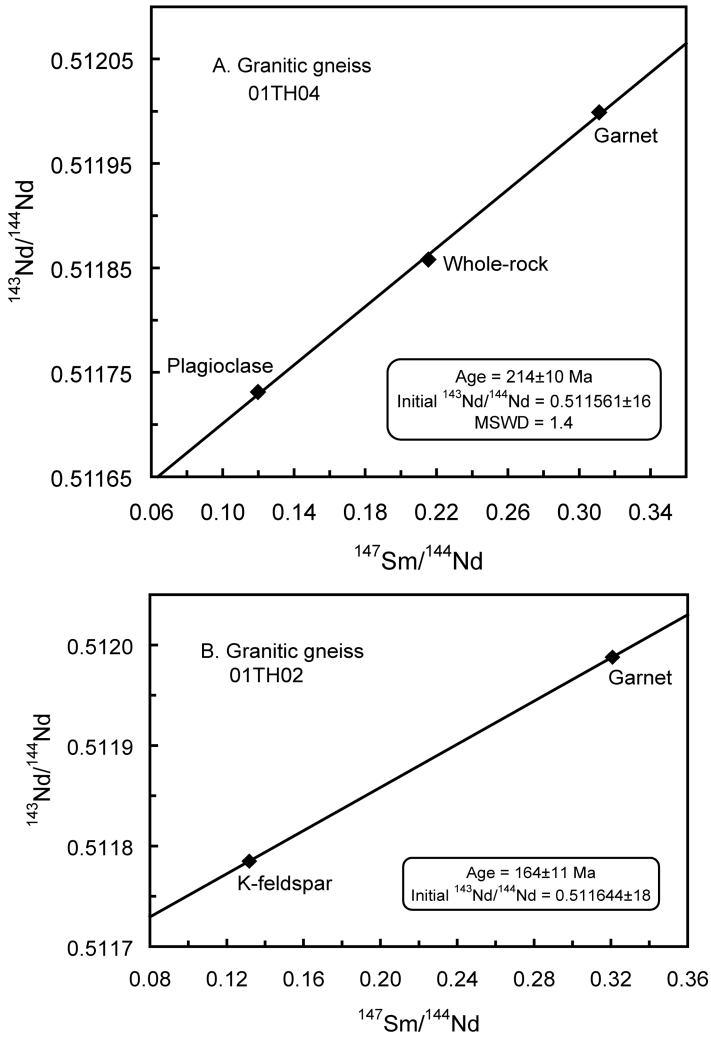

FIG. 8. Mineral Sm-Nd isochron plot for granitic gneisses from Taohang, Sulu orogen.

signature for crystalline zircon by O diffusion resetting during water-rock interaction depends on temperature, grain size, and duration. Under most geological circumstances, rates of O diffusion in zircon are so slow that small zircons of 30–50 μm grain size need over tens of millions of years to achieve isotopic reequilibration during subsolidus hydrothermal alteration or anhydrous high-T granulite-facies metamorphism, and thus will not experience significant change in $\delta^{18}O$ (Zheng et al., 2004).

Although crystalline zircon can survive subsolidus water-rock interaction (Zheng et al., 2004), metamict zircon may suffer O isotope resetting by diffusion at subsolidus temperatures (Cherniak and Watson, 2003; Valley, 2003). For the Taohang UHP metamorphic rocks, not only the CL imaging shows the typical structure of magmatic zoning for the zircons (Fig. 6), but also the zircon U-Pb dating gives the mid-Neoproterozoic age for the protoliths of the granitic orthogneiss (Fig. 7). This indicates that the zircons from the Taohang UHP metamorphic rocks are crystalline rather than metamict despite the presence of very thin (<10 μm) structureless rims of weak luminescence on some grains due to

metamorphic overgrowth. Because the zircons from the UHP metamorphic rocks at Taohang underwent only relatively "dry" granulite-facies overprinting (Yao et al., 2000), the zircon $\delta^{18}O$ values can reflect the O isotope composition of the protolith before the Triassic subduction, and thus point to low-^{18}O magmas from which the zircons crystallized (Zheng et al., 2004). Therefore, the low $\delta^{18}O$ zircons did not result from subsolidus hydrothermal alteration or anhydrous high-T metamorphism, but were crystallized from Neoproterozoic low $\delta^{18}O$ magmas. The Neoproterozoic low $\delta^{18}O$ magmas in turn resulted from remelting of low $\delta^{18}O$ materials—i.e., isotopic exchange between source rock and surface fluid (meteoric water or seawater) at high temperatures before remelting (Zheng et al., 2004).

The zircon U–Pb dates at 770 ± 23 Ma from this study and at 771 ± 9 Ma from Zheng et al. (2004) were acquired for protoliths of the granitic orthogneiss at Taohang (Fig. 7), consistent with protolith ages of 758 ± 15 Ma for protoliths of meta-igneous rocks from the other regions in the Dabie–Sulu orogenic belt (Zheng et al., 2004). This corresponds to mid-Neoproterozoic rift magmatism along the northern edge of the South China Block in response to breakup of the supercontinent Rodinia (Ames et al., 1996; Gao et al., 1996; Hacker et al., 1998; Zheng et al., 2004, 2006). Thus ^{18}O depletion in the protoliths of the granitic gneiss from Taohang is correlated with meteoric-hydrothermal alteration triggered by this mid-Neoproterozoic rift magmatism. During Triassic subduction, UHP metamorphism, and exhumation, the low $\delta^{18}O$ values acquired during the Neoproterozoic hydrothermal alteration and low-^{18}O magmatism were retained.

Fluid in deeply subducted continental crust

Compared to oceanic crust, the continental crust that was subducted to mantle depths and underwent UHP eclogite-facies metamorphism is relatively poor in water (Liou et al., 1997; Fu et al., 2001; Zheng et al., 2003a). Nevertheless, minor amounts of hydroxyl-bearing minerals such as phengite, epidote, and biotite occur as matrix or as mineral inclusions in the coesite-bearing rocks from Taohang (Yao et al., 2000; Ye et al., 2000), implying that they may be stable at UHP conditions and thus can store significant amounts of H_2O from premetamorphic protoliths at mantle depths (Zheng et al., 2003a).

Furthermore, nominally anhydrous minerals such as omphacite, garnet, and rutile under mantle conditions may contribute water to hydration and symplectization during retrograde metamorphism of the UHP rocks (Zheng et al., 1999, 2003a). It is well known that pyroxene, garnet, and rutile in eclogites can contain considerable amounts (tens to hundreds or even thousands of ppm) of water in the form of OH in their crystal structures at mantle pressures (Smyth et al., 1991; Bell and Rossman, 1992; Thompson, 1992; Rossman, 1996; Ingrin and Skogby, 2000). For example, minerals in the UHP eclogites from the Dabie-Sulu orogenic belt contain significant amounts of hydroxyl, about 115 to 1300 ppm H_2O in omphacite, 92 to 1735 ppm H_2O in garnet, and 4300 to 9600 ppm H_2O in rutile (Zhang et al., 2001, 2004; Xia et al., 2005). Clusters of water molecules were observed in garnet (Su et al., 2002). It is possible that the nominally anhydrous minerals containing OH behave isotopically like hydroxyl-bearing minerals in geochemical processes, and thus considerable O isotope fractionations may take place between OH and the anhydrous silicates.

TCEA-MS analysis in this study has detected significant amounts of H_2O in nominally anhydrous minerals from the UHP eclogite and granitic gneiss at Taohang in the Sulu orogen (Table 2). The bulk H_2O concentrations are 1278 to 1845 ppm in omphacite, 531 to 1539 ppm in garnet, 1620 to 1764 ppm in rutile, 351 to 2646 ppm in quartz, 711 to 1557 ppm in feldspars, 3987 to 4617 ppm in magnetite, 4041 ppm in titanite, and 882 ppm in apatite. Higher H_2O concentrations occur in garnet from the granitic gneiss than from the eclogite (Fig. 5), which may be the basic reason why no UHP index mineral like coesite can survive in UHP metagranites during exhumation. Such minor accessory minerals as magnetite, titanite, and rutile are usually considered to be refractory and thus resistant to O diffusion (Zheng and Fu, 1998), but significant amounts of H_2O are detected in them (Fig. 5). Rates of O isotope exchange of these minor minerals with matrix minerals could be enhanced by diffusion in the presence of water within them during exhumation or later events. This also explains why the mineral-pair O isotope geothermometry gave temperatures in Table 1 that are lower than those expected from their rates of O diffusion even during slow cooling.

TCEA-MS H isotope analysis for the hydroxyl-bearing minerals for the Taohang rocks shows variable δD values of –101 to –77‰ for muscovite and –62‰ for epidote (Table 2). These fall in the δD range of –127 to –49‰ determined by conventional extraction methods for hydroxyl-bearing minerals from UHP metamorphic rocks in the western part of

the Sulu orogen (Rumble and Yui, 1998; Zheng et al., 1998). At thermodynamic equilibrium, mica is expected to have higher δD values than epidote (Suzuoki and Epstein, 1976; Graham et al., 1980). What is observed from this study is D enrichment in epidote relative to muscovite (Table 2). Similar observations were also made by conventional methods for UHP eclogite and gneiss in the Dabie-Sulu orogenic belt (Fu et al., 1999; Zheng et al., 1999). This is a kind of H isotope disequilibrium that is ascribed to differential exchange of H isotopes with retrograde fluid during exhumation (Zheng et al., 2003a), because rates of H isotope exchange by diffusion in micas are slower than those in epidote (Table 5 and Fig. 9A). Disequilibrium O isotope fractionation also occurs in some of quartz-feldspar pairs from the granitic gneiss (Table 1). This is also attributable to differential exchange of O isotopes in the feldspars with retrograde fluid during exhumation because rates of O isotope exchange by hydrous diffusion in feldspars are much faster than those in quartz (Zheng and Fu, 1998).

More importantly, the similar δD values were also measured in this study for the nominally anhydrous minerals with –119 to –99‰ for omphacite, –106 to –77‰ for garnet, –121 to –97‰ for rutile, –78 to –58‰ for quartz, –73 to –68 for feldspars, –113 to –96‰ for magnetite, –82 for titanite, and –69‰ for apatite (Table 2). These new data confirm the previous conclusion that meteoric water was incorporated into the protoliths of UHP metabasite and metagranite before continental subduction (Zheng et al., 2003a). In addition, the bulk H_2O in nominally anhydrous minerals exhibits similar behavior of H isotope fractionation as that in hydroxyl-bearing minerals. This suggests that OH predominates in the analyzed H_2O from nominally anhydrous minerals. Experimental studies of H diffusion in such phases suggest the following sequence of rates: garnet < orthopyroxene < feldspar < quartz ≤ clinopyroxene < rutile (Table 5 and Fig. 9B). It appears that differential exchange of H isotopes also occurred between the nominally anhydrous minerals and the retrograde fluid during exhumation. In this regard, caution must be taken when discussing H isotope fractionations between OH in nominally anhydrous minerals and hydrous minerals with respect to their contribution to the D/H fractionation in mantle-derived minerals.

Taohang UHP metamorphic rocks were subjected to amphibolite-facies retrogression during exhumation (Yao et al., 2000). The O isotope composition of less refractory minerals provides a useful constraint on the origin of the retrograde fluid. Muscovite-rutile pairs from the eclogite yield isotopic temperatures of 380 to 450°C (Fig. 4) and quartz-feldspar pairs from the granitic gneiss yield isotopic temperatures of 200 to 515°C (Figs. 2 and 3). These suggest that the retrograde minerals achieved and preserved O isotope reequilibration under lower amphibolite-facies conditions. No O isotope shift is observed for refractory minerals from the eclogite and granitic gneiss. This suggests that the retrograde fluid was either in, or very close to, isotopic equilibrium with minerals in the UHP metamorphic rocks (Zheng et al., 1999). Therefore, the retrograde fluid would be internally buffered in terms of stable isotope compositions (Zheng et al., 1999, 2003a). This is also a kind of deuteric fluid that is cognate and evolved from within the system. Nevertheless, it remains an open question whether such low $\delta^{18}O$ and δD fluid was derived from decompressional exsolution of structural hydroxyl dissolved in UHP metamorphic minerals.

With subduction of continental crust to mantle depths, water could be incorporated as OH into anhydrous minerals (e.g., omphacite, garnet, and rutile) and hydroxyl-bearing minerals (e.g., phengite). During UHP metamorphism, the water in the form of hydroxyls is immobile in both anhydrous and hydroxyl-bearing minerals. A number of experimental investigations have shown that hydroxyl solubility in nominally anhydrous minerals decreases with decreasing pressure (Lu and Keppler, 1997; Withers et al., 1998; Mosenfelder, 2000; Rauch and Keppler, 2002; Koch-Muller et al., 2003; Bromiley et al., 2004; Mierdel and Keppler, 2004). UHP eclogites from Kokchetav in Kazakstan show that OH contents in clinopyroxene increase with pressure—i.e., 1110 to 1030 ppm in quartz-eclogite, 2430 to 1690 ppm in coesite-eclogite, and 3020 ppm in diamond-grade eclogite (Katayama and Nakashima, 2003). A linear increase in water content of omphacite and garnet with pressure is observed from the Kokchetav eclogite (Katayama et al., 2006). Thus as previously suggested by Zheng et al. (1999, 2003a), the solubility of hydroxyl in nominally anhydrous minerals decreases rapidly with abruptly decreasing pressure in the early stage of UHP slab exhumation, resulting in release of the significant amounts of aqueous fluid. Thus as pressure decreases due to slab uplift, hydroxyl in the anhydrous minerals could be released to react with host minerals, resulting in dissolution and

TABLE 5. Arrhenius Parameters for Hydrogen Diffusion in Minerals

Mineral	Abbr.	Z_T	Orientation	T (^{0}C)	P (MPa)	E (kJ/mol)	$\ln D_0$ (cm^2/sec)	Reference
				Hydroxyl-bearing minerals				
Biotite	Bt	50.15	//c	450–800	100	116.3	–14.89	Suzuoki and Epstein, 1976
Biotite[1]	Bt	50.15	⊥c	450–800	100	122.6	–7.18	Suzuoki and Epstein, 1976
Epidote	Ep	45.73	⊥c	200–350	200–400	128	0.21	Graham, 1981
Epidote	Ep	45.73	powder	450–650	200, 400	57.7	–12.62	Graham, 1981
Epidote	Ep	45.73	//c	200–350	200–400	128.5	2.23	Graham, 1981
Epidote[1]	Ep	45.73	//c	450–650	400	52.3	–11.54	Graham, 1981
Hornblende[1]	Hbl	50.54	//c	350–550	100	79.5	–15.66	Graham et al., 1984
Hornblende	Hbl	50.54	⊥c	350–550	100	84.1	–17.55	Graham et al., 1984
Muscovite	Ms	51.50	//c	450–750	200, 400	119.7	–16.12	Graham, 1981
Muscovite[1]	Ms	51.50	⊥c	450–750	200, 400	121.3	–9.16	Graham, 1981
Phlogopite	Phl	49.70	//c	575–650	100	128.6	–14.06	Suzuoki and Epstein, 1976
Phlogopite[1]	Phl	49.70	⊥c	575–650	100	155.2	–3.80	Suzuoki and Epstein, 1976
Tremolite[1]	Tr	52.46	//c	350–800	200–400	72.4	–15.55	Graham et al., 1984
Tremolite	Tr	52.46	//c	650–850	200–400	71.1	–18.54	Graham et al., 1984
Zoisite	Zo	45.84	//c	350–650	200–400	100	–8.73	Graham, 1981
Zoisite	Zo	45.84	powder	350–650	200, 400	102.5	–10.02	Graham, 1981
Zoisite	Zo	45.84	⊥c	200–650	200–400	52.3	–10.34	Graham et al., 1980
Zoisite[1]	Zo	45.84	//c	200–650	200–400	52.3	–8.66	Graham et al., 1980
				Nominally anhydrous minerals				
Adularia[1]	Adl	53.91	plate	500–900	0.1	172 ± 15	1.82	Kronenberg et al. (1996)
Diopside	Di	46.43	//(001), (100), (010)	700–1000	0.1	136 ± 27	–5.39	Ingrin et al. (1995)
Diopside	Di	46.43	//(100)	700–850	0.1	181 ± 38	4.37	Woods et al., 2000
Diopside	Di	46.43	//(001)	700–850	0.1	153 ± 32	1.38	Woods et al., 2000
Diopside[1]	Di	46.43	//(001) and (100)	600–900	0.1	149 ± 16	1.38	Hercule and Ingrin, 1999
Diopside	Di	46.43	//(010)	600–900	0.1	143 ± 33	–2.30	Hercule and Ingrin, 1999
Enstatite	En	49.78	//(100) and (010)	700, 900	0.1	295 ± 55	9.52	Stalder and Skogby, 2003
Orthopyroxene[1]	Opx	51.00	//(001), (100), (010)	700, 1000	0.1	213 ± 47	5.19	Stalder and Skogby, 2003

Pyrope	Prp	39.87		700-950	0.1	254 ± 12	9.78	Wang et al., 1996
Pyrope	Prp	39.87		700–950	0.1	241 ± 32	9.52	Wang et al., 1996
Pyrope[1]	Prp	39.87	Single crystal	700–950	2700	140 ± 38	–6.45	Blanchard and Ingrin, 2004a
Pyrope	Prp	39.87	Single crystal	800–1050	$pO_2 = 0.21$ atm	277 ± 22	8.06	Blanchard and Ingrin, 2004b
Pyrope	Prp	39.87	Single crystal	800–1050	$pO_2 = 10^{-16}$ atm	329 ± 21	11.28	Blanchard and Ingrin, 2004b
β-Quartz[1]	β-Qz	61.62	//c	700–900	890–1550	200 ± 20	7.24	Kronmberg et al., 1996
α-Quartz[1]	α-Qz	59.89	//c	400–620	2.5	79.5	–9.90	Kats et al., 1962
β-Quartz	β-Qz	61.62	//c	700–900	2.5	175.7	1.61	Kats et al., 1962
β-Quartz	β-Qz	61.62	//c	720–850	0.06	93.7	–15.09	Shaffer et al., 1974
β-Quartz	β-Qz	61.62	//c	721–850	0.06	100	–14.26	Shaffer et al., 1974
β-Quartz	β-Qz	61.62	//c	722–850	0.06	104.2	–13.91	Shaffer et al., 1974
β-Quartz	β-Qz	61.62	//c	723–850	0.06	108.4	–13.98	Shaffer et al., 1974
Rutile[1]	Rt	45.66	//c	550–700	0.1	123.4	–0.97	Paek, 1974
Rutile	Rt	45.66	⊥c	302–550	0.1	56.9	–6.32	Paek, 1974

[1]Denotes the diffusion data used in Figure 5.

recrystallization. Therefore, retrograde fluid active during exhumation of the UHP metamorphic rocks at Taohang was internally buffered and came from the subducted continent itself.

Both the O isotope disequilibrium in Qz-Pl and Qz-Kfs pairs and the anomalously low $\delta^{18}O$ values for the feldspars occur in some samples of the Taohang granitic gneiss. This suggests that water-rock interaction occurred between the granitic gneisses and the low $\delta^{18}O$ fluid at a stage after the amphibolite-facies retrogression (a later event). Under the binocular microscope, the grains of plagioclase and K-feldspar are coarse and have granitic metacrystal texture. This indicates that plagioclase and K-feldspar did not experience recrystallization by exotic fluid infiltration. Thus the mechanism for change in $\delta^{18}O$ values for the feldspars was diffusion-controlled exchange of O isotopes rather than surface reaction-controlled process. Structural hydroxyl in hydroxyl-bearing silicates is depleted in ^{18}O relative to the framework of anhydrous silicates (Zheng, 1993b). Thus the accumulation of hydroxyl liberated from nominally anhydrous minerals could have formed the low $\delta^{18}O$ and δD retrograde fluid either during the initial exhumation or in the post-collisional phase. The liberation process itself proceeded by hydroxyl diffusion and thus was associated with O and H isotope exchange with the feldspars.

The petrological study by Yao et al. (2000) indicates a transition from eclogite-facies to granulite-facies paragenesis in the coesite-bearing eclogite. A temperature increase is required to trigger this transition, resulting in dehydration of the eclogite-facies rocks. Amphibolite-facies retrogression of the granitic gneiss is also evident (Ye et al., 2000), pointing to hydration in some of the UHP rocks. Thus it remains to resolve whether there is a causal link between dehydration during the granulite-facies metamorphism and hydration during amphibolite-facies retrogression. In other words, did the aqueous fluid liberated by the granulite-facies metamorphism provide a retrograde fluid source for the amphibolite-facies overprinting? If so, it is also interesting to know whether this dehydration-hydration link took place during exhumation or in the post-collisional period. Because fluid is an important medium for element and isotope exchange to achieve thermodynamic equilibrium, its presence or absence plays a critical role in dictating the attainment, preservation or destruction, and reequilibration of geochronometric and geothermometric systems in metamorphic minerals (Zheng et al., 2003c).

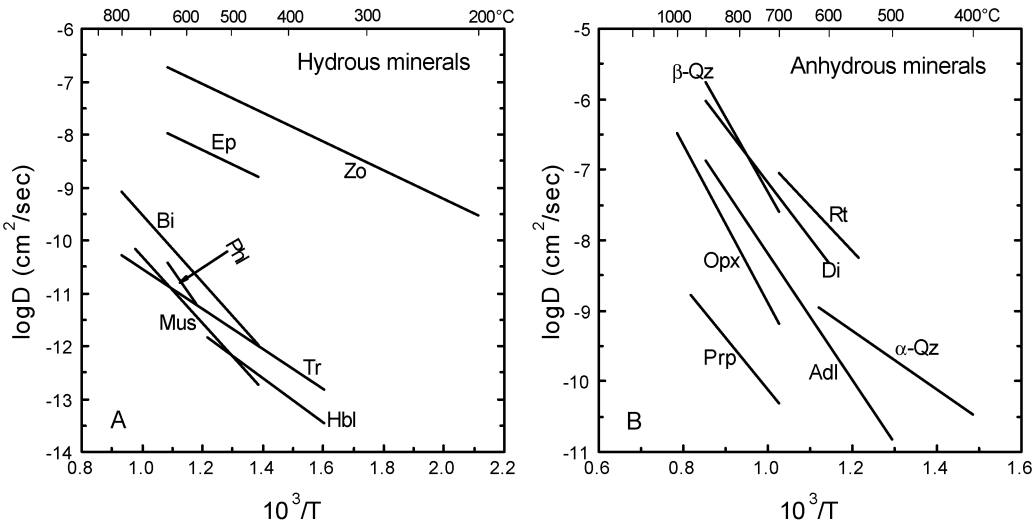

FIG. 9. Comparison of H diffusivity in minerals (data from Table 5 with asterisk)

TABLE 6. Compilation of Sm-Nd and O Diffusion Coefficients and Closure Temperatures for Minerals

Mineral	Element	$\ln D_0$, cm^2/s	E, KJ/mol	Closure temperature, T, °C[1]	Reference
Almandine	O (dry)	3.15	474	964	Zheng and Fu, 1998
	O (wet)	–9.72	301±46	654 ~ 971	Coughlan, 1990
	Nd (wet)	–19.59	184	666	Coughlan, 1990
	Sm-Nd (dry)	–9.97	258	671	Ganguly et al., 1998
Anorthite	O (dry)	–12.9	174	437	Zheng and Fu, 1998
	O (wet)	–14.98	128	299	Zheng and Fu, 1998
	Nd (dry)	–2.83	398	918	Cherniak, 2003
Orthoclase	O (dry)	–15.71	121	283	Zheng and Fu, 1998
	O (wet)	–16.91	107	246	Zheng and Fu, 1998
Albite	O (dry)	–12.84	175	440	Zheng and Fu, 1998
	O (wet)	–14.94	129	302	Zheng and Fu, 1998
Oligoclase	Nd (dry)	3.14	425	840	Cherniak, 2003

[1]T calculated by using the formula of Dodson (1979) under the assumptions of a = 0.1 mm, dT/dt = 10°C/Ma, and A = 8.7.

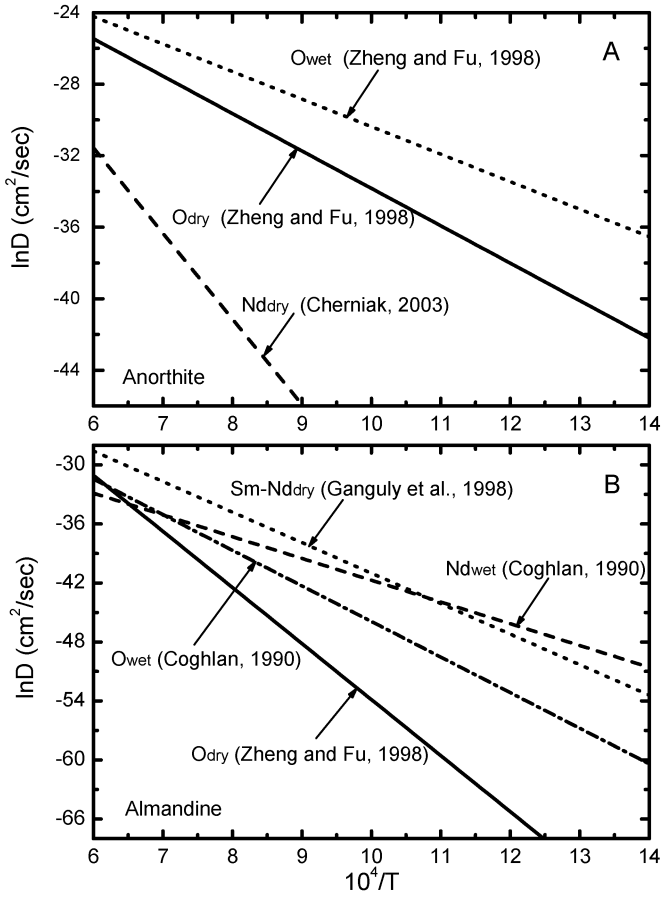

FIG. 10. Comparison of O and Sm-Nd diffusivities in different minerals (data from Table 6)

Oxygen Isotope Constraints on the Sm-Nd Chronometer

Rates of Sm-Nd and O diffusion in metamorphic minerals are comparable in many cases (Zheng et al., 2002, 2003c). An inspection of diffusion data available for Nd and O in minerals (Table 6 and Fig. 10) show that Sm and Nd have diffusion rates slower than O in some minerals, but similar to or faster than O in other minerals. Therefore, O isotope equilibrium between coexisting minerals can serve as a guide to evaluate whether Nd isotopic equilibrium existed under the same conditions (Zheng et al., 2002, 2003b, 2003c; Xie et al., 2004). For example, rates of O diffusion in feldspar are much faster than those of Nd diffusion. If O isotope equilibrium involving feldspar was disturbed by a later process (e.g. retrograde metamorphism, hydrothermal alteration, etc.), the mineral Sm-Nd chronometric system might remain undisturbed. On the other hand, attainment of isotopic equilibrium in a mineral Sm-Nd system would suggest achievement of O isotope equilibrium in feldspar.

As shown in Figure 11, the O isotopic temperatures for quartz-garnet pairs in the granitic gneiss are 670°C for sample 01TH02 and 685°C for sample 01TH04, indicating that these pairs achieved and preserved O isotope equilibrium under eclogite-facies conditions. The O isotopic temperatures for the quartz-plagioclase and quartz-K-feldspar pairs in sample 01TH04 are 355°C and 405°C, respectively (Fig. 11). This indicates that the

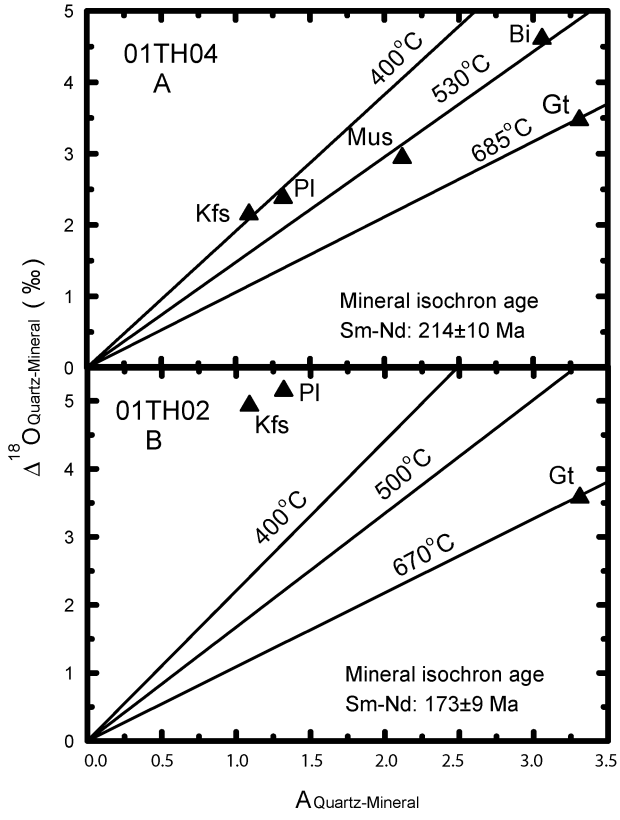

FIG. 11. Isotherm plot for O isotope fractionations between quartz and other minerals for Sm-Nd isochron dating granitic gneisses at Taohang, Sulu orogen.

quartz-feldspar pairs achieved and preserved O isotope re-equilibration under lower amphibolite-facies conditions.

The mechanism of O isotope exchange between minerals is diffusion-dominant during high-grade metamorphism (Giletti, 1985; Cole and Ohmoto, 1986; Cole and Chakraborty, 2001). As shown in Figure 10 and Table 6, the diffusion rates of O in garnet are slower than those of Nd diffusion and the closure temperatures of O diffusion are higher than those of the Sm-Nd system under the same conditions of dry metamorphism. For granitic gneiss 01TH04, the O isotopic temperature of 685°C (Fig. 11A) for the quartz-garnet pair suggests that O isotopes involving garnet achieved and preserved thermodynamic equilibrium under eclogite-facies conditions, and thus the Sm-Nd system in garnet achieved isotopic equilibrium under the same conditions. Using the formula of Dodson (1979), the closure temperatures of O and Nd diffusion in garnet and feldspar are calculated and listed in Table 6. The closure temperatures of 654 to 971°C for the Sm and Nd diffusion in garnet indicate that the Sm-Nd system in garnet achieved isotopic equilibrium during eclogite-facies metamorphism, and was closed during cooling subsequent to the eclogite-facies metamorphism.

As shown in Figure 10A and Table 6, the rates of O diffusion in feldspar are much faster than those of Nd diffusion, and the closure temperatures of Sm-Nd diffusion are higher than those of O under the same conditions of metamorphism. For granitic gneiss 01TH04, the O isotopic temperatures for the quartz-plagioclase and quartz-K-feldspar pairs are 355°C and 405°C, respectively (Fig. 11A). This indicates that the O isotope composition of feldspars was reset, but re-equilibrated at lower temperatures than amphibolite-facies conditions. O isotope equi-

librium involving feldspar is very susceptible to fluid disturbance (Cole and Ohmoto, 1986; Cole and Chakraborty, 2001). Thus, the O isotope system in feldspars from sample 01TH04 could become open by a later event. The closure temperatures of 840 to 918°C for the Sm-Nd radiometric system in feldspar are much higher than the O isotopic temperatures of 355 to 405°C for quartz-feldspar pairs. These observations suggest that the Sm-Nd system, which achieved isotopic equilibrium in feldspar during the eclogite-facies metamorphism, was closed after the eclogite-facies metamorphism and not disturbed by later geological processes. Therefore, Sm-Nd isotope data for the garnet–plagioclase–whole rock assemblage from granitic gneiss 01TH04 define the geologically meaningful isochron age of 214 ± 10 Ma (Fig. 8A). Because fluid release is expected to occur by hydroxyl exsolution during initial exhumation from the UHP phase to the HP eclogite-facies (Zheng et al., 2003a), fluid-present recrystallization should take place at this state, resulting in both mineral Sm-Nd and O isotopic re-equilibration. On the other hand, the SHRIMP zircon U-Pb age of 227 ± 3 Ma was dated by Zheng et al. (2004) for the Taohang granitic gneiss. This age agrees with SHRIMP U-Pb ages for coesite-bearing domains of zircon from the granitic gneiss at Donghai in the southeastern part of the Sulu orogen (Liu et al., 2004a, 2004b). In this regard, the Sm-Nd isochron age, together with the zircon U-Pb age of 214 ± 9 Ma, is interpreted to register the timing of HP eclogite-facies recrystallization.

As shown in Figure 11B and Table 1, in contrast, great fractionations of 4.93 to 5.15‰ are obtained between quartz and feldspar from granitic gneiss 01TH02, suggesting that O isotope disequilibrium characterizes this mineral pair. Even the negative $\Delta^{18}O$ value of –1.35‰ occurs between coexisting K-feldspar and garnet. The low $\delta^{18}O$ values for the K-feldspar and plagioclase indicate that the O isotope system in the feldspars was disturbed by a low $\delta^{18}O$ fluid at medium to high temperatures because low-T alteration will increase mineral $\delta^{18}O$ values. It remains to determine if the granulite-facies dehydration delivered the low $\delta^{18}O$ fluid for the hydrothermal alteration. On the other hand, the quartz-garnet pair yields an O isotope temperature of 670°C, suggesting that secondary disturbance would have taken place at medium-T temperatures somewhere between 600°C and 400°C. Although the rates of isotope exchange by Sm and Nd diffusion in garnet are sluggish enough to prohibit the secondary resetting, the secondary disturbance resulting in the O isotope disequilibria concerning the feldspars implies that the whole-rock Sm-Nd isotope composition may be reset by moderate-T water-rock interaction, resulting in the decreased Sm-Nd isochron age of 164 ± 11 Ma for the association of garnet and K-feldspar (Fig. 8B). In this regard, O isotope disequilibrium provides a test of the invalidity of the Sm-Nd chronometer in this case. Furthermore, disequilibrium O isotope fractionation suggests limited fluid activity in the post-collisional stage.

Conclusions

UHP eclogite and granitic gneiss from Taohang show heterogeneous ^{18}O-depletion on an outcrop scale. Most minerals from the UHP metamorphic rocks achieved and preserved O isotope equilibrium and re-equilibration acquired from eclogite-facies metamorphism to lower amphibolite-facies retrogression. Zircons with low $\delta^{18}O$ values of –1.3 to 4.2‰ have large magmatic cores and very thin (< 10 μm) rims of metamorphic overgrowth. U-Pb discordia dating for low $\delta^{18}O$ zircons yield mid-Neoproterozoic ages of ~770 Ma for the protolith of granitic orthogneiss, consistent with protolith ages of UHP meta-igneous rocks from other regions in the Dabie-Sulu orogenic belt. Because zircons from Taohang UHP metamorphic rocks suffered only relatively "dry" eclogite-facies metamorphism, the $\delta^{18}O$ values for zircons reflect the O isotope compositions of protolith magmas from which they crystallized. The low $\delta^{18}O$ zircons crystallized from Neoproterozoic low $\delta^{18}O$ magmas which experienced meteoric-hydrothermal alteration prior to remelting in an active rift setting.

TCEA-MS techniques have been successfully applied to analyses of both H isotope compositions and H_2O concentrations in hydrous and nominally anhydrous minerals from Taohang UHP metamorphic rocks. Results show variable δD values of –121 to –58‰ for such nominally anhydrous minerals as omphacite, garnet, rutile, and quartz in the eclogite, as well as feldspars, quartz, magnetite, titanite, and apatite in the granitic gneiss. Similar δD values of –101 to –62‰ were also obtained for the hydroxyl-bearing minerals muscovite and epidote. These δD values are consistent with previous measurements by conventional extraction methods, indicating incorporation of meteoric water into protoliths of UHP meta-igneous rocks by high-T alteration and

remelting. More importantly, hundreds to thousands of ppm H_2O were detected in nominally anhydrous minerals, with similar behaviors of H isotope fractionation to those in hydroxyl-bearing minerals. Therefore, besides hydrous minerals, nominally anhydrous minerals also control the distribution of water in deeply subducted continental crust.

Most minerals from both eclogite and granitic gneiss achieved and preserved O isotope reequilibration under conditions of amphibolite-facies retrogression. Almost no O isotope shift is observed for refractory minerals from eclogite and granitic gneiss that experienced either granulite-facies or amphibolite-facies overprinting. This suggests that retrograde fluid was internally buffered and came from the interior of the subducted continent. The state of mineral O isotope equilibrium provides reasonable constraints on the validity of mineral Sm-Nd isochrons. Under closed-system conditions during UHP metamorphism, diffusion-controlled isotope exchange suggests that diffusion rates of O, Sm, and Nd in the same minerals are comparable. Thus O isotope equilibrium can serve as a test for validity of the mineral Sm-Nd isochron. A Sm-Nd isochron age of 214 ± 10 Ma was obtained for Gt-Wr-Pl from a granitic gneiss, and agrees with a zircon U-Pb age of 214 ± 9 Ma from the same rock suite. This age is interpreted as dating the mineral Sm-Nd re-equilibration by HP eclogite-facies recrystallization during the initial exhumation. Thus a fluid-present process is suggested for zircon overgrowth and isotopic reequilibration during this retrogression.

Oxygen isotope disequilibrium in a Gt-Kfs pair, and low $\delta^{18}O$ values for K-feldspar and plagioclase from another granitic gneiss indicate that the feldspars were disturbed by later infiltration of a low $\delta^{18}O$ fluid. Under open-system conditions at medium temperatures (600 to 400ºC), even if minerals were disturbed by reaction with an exotic fluid, rates of isotope exchange are still comparable between O and Sm-Nd diffusion in feldspars. Thus a Gt-Kfs Sm-Nd isochron age of 164 ± 11 Ma corresponds to the state of O isotope disequilibrium between garnet and K-feldspar. The Middle Jurassic age is significantly later than that of the Triassic collision orogeny, and thus has no relevance to the processes of both continental subduction and exhumation. The disequilibrium O isotope fractionation suggests limited fluid activity in the post-collisional stage. This provides a test for invalidity of the mineral Sm-Nd chronometer in the disequilibrium assemblage.

Acknowledgments

This study was supported by funds from the Natural Science Foundation of China (40573011) and the National Ministry of Science and Technology (2003CB716501). We appreciate the assistance of J.-X. Zhou and Z.-Y. Chen with CL imaging, S. Gao and H.-L. Yuan with LA-ICP-MS dating, and Y.-B. Zhao and X.-P. Zha with O isotope analyses. Thanks are due to P. Philippot and M. Thoeni for their constructive comments that result in significant improvement of the manuscript.

REFERENCES

Ames, L., Zhou, G.-Z., and Xiong, B.-C., 1996, Geochronology and isotopic charater of ultrahigh-pressure metamorphism with implication for collision of the Sino-Korean and Yangtze cratons, central China: Tectonics, v. 15, p. 472–489.

Anderson, T., 2002, Correction of common lead in U-Pb analyses that do not report ^{204}Pb: Chemical Geology, v. 192, p. 59–79.

Ayers, J. C., Dunkle, S., Gao, S., and Miller, C. E., 2002, Constraints on timing of peak and retrograde metamorphism in the Dabie Shan ultrahigh-pressure metamorphic belt, east-central China, using U-Th-Pb dating of zircon and monazite: Chemical Geology, v. 186, p. 315–331.

Baker, J., Matthews, A., Mattey, D., Rowley, D., and Xue, F., 1997, Fluid-rock interactions during ultra-high pressure metamorphism, Dabie Shan, China: Geochimica et Cosmochimica Acta, v. 61, p. 1658–1696.

Begley, I. S., and Scrimgeour, C. M., 1997, High-precision δ^2H and $\delta^{18}O$ measurement for water and volatile organic compounds by continuous-flow pyrolysis isotope ratio mass spectrometry: Analytical Chemistry, v. 69, 1530–1535.

Bell, D. R. and Rossman, G. R., 1992, Water in the Earth's mantle: The role of nominally anhydrous minerals: Science, v. 255, p. 1391–1397.

Blanchard, M., and Ingrin, J., 2004a, Kinetics of deuteration in pyrope: European Journal of Mineralogy, v. 16, p. 567–576.

Blanchard, M. and Ingrin, J., 2004b, Hydrogen diffusion in Dora Maira pyrope: Physics and Chemistry of Minerals, v. 31, p. 593–605.

Bromiley, G. D., Keppler, H., McCammon, C., Bromiley, F. A., and Jacobsen, S. D., 2004, Hydrogen solubility and speciation in natural, gem-quality chromian diopside: American Mineralogist, v. 89, p. 941–949.

Burgoyne, T. W., and Hayes, J. M., 1998, Quantitative production of H_2 by pyrolysis of gas chromatographic effluents: Analytical Chemistry, v. 70, p. 5136–5141.

Chavagnac, V. and Jahn, B.-m., 1996, Coesite-bearing eclogites from the Bixiling Complex, Dabie Mountains, China: Sm-Nd ages, geochemical characteristics, and tectonic implications: Chemical Geology, v. 133, p. 29–51.

Cherniak, D. J., 2003, REE diffusion in feldspar: Chemical Geology, v. 193, p. 25–41.

Cherniak, D. J., and Watson, E. B., 2003, Diffusion in zircon, *in* Hanchar, J. M., and Hoskin, P. W. O., eds., Zircon: Experiments, isotopes, and trace element investigations: Washington, DC, Mineralogical Society of America, Reviews in Mineralogy and Geochemistry, v. 53, p. 113–143.

Cole, D. R. and Chakraborty, S., 2001, Rates and mechanisms of isotopic exchange, *in* Valley, J. W., and Cole, D. R., eds., Stable isotope geochemistry: Reviews in Mineralogy and Geochemistry, v. 43, Mineralogical Society of America, Washington, DC, p. 83–233.

Cole, D. R. and Ohmoto, H., 1986, Kinetics of isotopic exchange at elevated temperatures and pressures, *in* Valley, J. W., Taylor, H. P., Jr., and O'Neil, J. R., eds., Stable isotopes in high-temperature geological processes: Washington, DC, Mineralogical Society of America, Reviews in Mineralogy, v. 16, p. 41–90.

Cong, B., 1996, Ultrahigh-pressure metamorphic rocks in the Dabieshan-Sulu Region of China: Beijing, China and London, UK, Science Press and Kluwer Academic Publishers, 224 p.

Coughlan, R. A. N., 1990, Studies in diffusion transport: Grain boundary transport of oxygen in feldspars, strontium, and the REEs in garnet, and thermal histories of granitic intrusions in south-central Maine using oxygen isotopes: Unpubl. Ph.D thesis, Brown University, Providence, Rhode Island.

Dodson, M. H., 1979, Theory of cooling age, *in* Jaeger, E., and Hunziker, J. C., eds., Lecture in isotope geology: Berlin, Germany, Springer-Verlag, p. 194–202.

Eiler, J. M., Farley, K. A., Valley, J. W., Hofmann, A. W., and Stolper, E. M., 1996, Oxygen isotope constraints on the sources of Hawaiian volcanism: Earth and Planetary Science Letters, v. 144, p. 453–468.

Eiler, J. M., and Kitchen, N., 2001, Hydrogen-isotope analysis of nanomole (picoliter) quantities of H_2O: Geochimica et Cosmochimica Acta, v. 65, p. 4467–4479.

Ernst, W. G., and Liu, J. G., 1999, Overview of UHP metamorphism and tectonics in well-studied collisional orogens: International Geology Review, v. 41, p. 477–493.

Fu, B., Zheng, Y.-F., Wang, Z.-R., Xiao, Y.-L., Gong, B., and Li, S.-G., 1999, Oxygen and hydrogen isotope geochemistry of gneisses associated with ultrahigh pressure eclogites at Shuanghe in the Dabie Mountains: Contributions to Mineralogy and Petrology, v. 134, p. 52–66.

Fu, B., Touret, J. L. R., and Zheng, Y.-F., 2001, Fluid inclusions in coesite-bearing eclogites and jadeite at Shuanghe, DabieShan, China: Journal of Metamorphic Geology, v. 19, p. 529–545.

Ganguly, J., Tirone, M., and Hervig, R. L., 1998, Diffusional kinetics of samarium and neodymium in garnet, and a model for determining cooling rates of rocks: Science, v. 281, p. 805–807.

Gao, S., Zhang, B.-R., and Li, Z.-J., 1996, Geochemical evidence for Proterozoic tectonic evolution of the Qinling Orogenic Belt and its adjacent margins of North China and Yangtze Cratons: Precambrian Research, v. 80, p. 23–48.

Giletti, B. J., 1985, The nature of oxygen transport within minerals in the presence of hydrothermal water and the role of diffusion: Chemical Geology, v. 53, p. 197–206.

Godin, J. P., Richelle, M., Metairon, S., and Fay, L. B., 2004, [^{2}H/H] isotope ratio analyses of [$^2H_5$]cholesterol using high-temperature conversion elemental analyser isotope-ratio mass spectrometry: Determination of cholesterol absorption in normocholesterolemic volunteers: Rapid Communications in Mass Spectrometry, v. 18, p. 325–330.

Graham, C. M., Sheppard, S. M. F., and Heaton, T. H. E., 1980, Experimental hydrogen isotope studies: I. Systematics of hydrogen isotope fractionation in the systems epidote-H_2O, zoisite-H_2O, and AlO(OH)-H_2O: Geochimica et Cosmochimica Acta, v. 44, p. 353–364.

Graham, C. M., 1981, Experimental hydrogen isotope studies III: Diffusion of hydrogen in hydrous minerals, and stable isotope exchange in metamorphic rocks: Contributions to Mineralogy and Petrology, v. 76, p. 216–228.

Graham, C. M., Harmon, R. S., and Sheppard, S. M. F., 1984, Experimental hydrogen isotope studies: Hydrogen isotope exchange between amphibole and water: American Mineralogist, v. 69, p. 128–138.

Hacker, B. R., Ratschbacher, L., and Webb, L., 1998, U/Pb zircon ages constrain the architecture of the ultrahigh-pressure Qinling-Dabie orogen, China: Earth and Planetary Science Letters, v. 161, p. 215–231.

Hacker, B. R., Ratschbacher, L., Webb, L., McWilliams, M. O., Ireland, T., Calvert, A., Dong, S., Wenk, H. R., and Chateigner, D., 2000, Exhumation of ultrahigh-pressure continental crust in east central China: Late Triassic–Early Jurassic tectonic unroofing: Journal of Geophysics Research, v. 105B, p. 13,339–13,364.

Hercule, S., and Ingrin, J., 1999, Hydrogen in diopside: Diffusion, kinetics of extraction-incorporation, and solubility: American Mineralogist, v. 84, p. 1577–1587.

Hilkert, A. W., Douthitt, C. B., Schlueter, H. J., and Brand, W. A., 1999, Isotope ratio monitoring gas chromatography/mass spectrometry of D/H by high temperature conversion isotope ratio mass spectrometry: Rapid Communications in Mass Spectrometry, v. 13, p. 1226–1230.

Hoefs, J., 1997, Stable isotope geochemistry, 4th ed.: Berlin, Germany, Springer-Verlag, 201 p.

Ingrin, J., Hercule, S., and Charton, T., 1995, Diffusion of hydrogen in diopside: Results of dehydration experiments: Journal of Geophysical Research, v. 100B, v. 15,489–15,499.

Ingrin, J., and Skogby, H., 2000, Hydrogen in nominally anhydrous upper-mantle minerals: Concentration levels and implications: European Journal of Mineralogy, v. 12, p. 543–570.

Katayama, I., and Nakashima, S., 2003, Hydroxyl in clinopyroxene from the deep subducted crust: Evidence for H_2O transport into the mantle: American Mineralogist, v. 88, p. 229–234.

Katayama, I., Nakashima, S., and Yurimoto, H., 2006, Water content in natural eclogite and implication for water transport into the deep upper mantle: Lithos, v. 86, p. 245–259.

Kats, A., Haven, Y., and Stevels, J. M., 1962, Hydroxyl groups in β-quartz: Physics and Chemistry of Glasses, v. 3, p. 69–75.

Koch-Muller, M., Dera, P., Fei, Y. W., Reno, B., Sobolev, N., Hauri, E., and Wysoczanski, R., 2003, OH^- in synthetic and natural coesite: American Mineralogist, v. 88, p. 1436–1445.

Kronenberg, A. K., Yund, R. A., and Rossman, G. R., 1996, Stationary and mobile hydrogen defects in potassium feldspar: Geochimica et Cosmochimica Acta, v. 60, p. 4075–4094.

Li, S.-G., Jagoutz, E., Chen, Y.-Z. and Li, Q.-L., 2000, Sm-Nd and Rb-Sr isotopic chronology and cooling history of ultrahigh pressure metamorphic rocks and their country rocks at Shuanghe in the Dabie Mountains, Central China: Geochimica et Cosmochimica Acta, v. 64, p. 1077–1093.

Li, S.-G., Jagoutz, E., Lo, C.-H., Chen, Y.-Z., Li, Q.-L., and Xiao, Y.-L., 1999, Sm/Nd, Rb/Sr, and $^{40}Ar/^{39}Ar$ isotopic systematics of the ultrahigh-pressure metamorphic rocks in the Dabie-Sulu belt, Central China: A retrospective view: International Geology Review, v. 41, p. 1114–1124.

Li, X.-P., Zheng, Y.-F., Wu, Y.-B., Chen, F. K., Gong, B., Li, Y.-L., 2004, Low-T eclogite in the Dabie terrane of China: Petrological and isotopic constraints on fluid activity and radiometric dating: Contributions to Mineralogy and Petrology, v. 148, p. 443–470.

Li, Z.-C., Wan, J.-H., and Du, G.-M., 1988, Investigation on the experimental conditions for Sm-Nd dating and its applications in geology: Bulletin of Yichang Instutite of Geology and Mineralogy Resources, v. 13, p. 1–23 (in Chinese with English abstract).

Liou, J. G., and Zhang, R. Y., 1996, Occurrence of intergranular coesite in ultrahigh-pressure rocks from the Sulu region, eastern China: Implication for lack of fluid during exhumation: American Mineralogist, v. 81, p. 1217–1221.

Liou, J. G., Zhang, R. Y., and Jahn, B.-m., 1997, Petrology, geochemistry and isotope data on a ultrahigh-pressure jadeite quartzite from Shuanghe, Dabie Mountains, East-Central China: Lithos, v. 41, p. 59–78.

Liu, F. L., and Xu, Z. Q., 2004, Fluid inclusions hidden in coesite-bearing zircons in ultrahigh-pressure metamorphic rocks from southwestern Sulu terrane in eastern China: Chinese Science Bulletin, v. 49, p. 396–404.

Liu, F. L., Xu, Z. Q., Liou, J. G., and Song, B., 2004a, SHRIMP U-Pb ages of ultrahigh-pressure and retrograde metamorphism of gneisses, south-western Sulu terrane, eastern China: Journal of Metamorphic Geology, v. 22, p. 315–326.

Liu, F. L., Xu, Z. Q., and Xue, H. M., 2004b, Tracing the protolith, UHP metamorphism, and exhumation ages of orthogneiss from the SW Sulu terrane (eastern China): SHRIMP U-Pb dating of mineral inclusion–bearing zircons: Lithos, v. 78, p. 411–429.

Lu, R., and Keppler, H., 1997, Water solubility in pyrope to 100 kbar: Contributions to Mineralogy and Petrology, v. 129, p. 35–42.

Ludwig, K. R., 2001, Users manual for Isoplot/Ex (rev. 2.49): A geochronological toolkit for Microsoft Excel: Berkeley, CA, Berkeley Geochronological Center, Special Publication, No. 1a: 55 p.

Mierdel, K., and Keppler, H., 2004, The temperature dependence of water solubility in enstatite: Contributions to Mineralogy and Petrology, v. 148, p. 305–311.

Mosenfelder, J. L., 2000, Pressure dependence of hydroxyl solubility on coesite: Physics and Chemistry of Minerals, v. 27, p. 610–617.

Okay, A. I., Xu, S.-T., and Sengor, A. M. C., 1989, Coesite from the Dabieshan eclogites, Central China: European Journal of Mineralogy, v. 1, p. 595–598.

Paek, S. H., 1974, Diffusion of hydrogen and deuterium in rutile: Unpubl. Ph.D. dissertation, University of Utah.

Rauch, M. and Keppler, H., 2002, Water solubility in orthopyroxene: Contributions to Mineralogy and Petrology, v. 143, p. 525–536.

Rossman, G. R., 1996, Studies of OH in nominally anhydrous minerals: Physics and Chemistry of Minerals, v. 23, p. 299–304.

Rowley, D. B., Xue, F., Tucker, R. D., Peng, Z. X., Baker, J., and Davis, A., 1997, Ages of ultrahigh pressure metamorphism and protolith orthogneisses from the eastern Dabie Shan: U/Pb zircon geochronology: Earth and Planetary Science Letters, v. 151, p. 191–203.

Rumble, D., Giorgis, D., and Oreland, T., 2002, Low $\delta^{18}O$ zircons, U-Pb dating, and the age of Qinglongshan oxygen and hydrogen isotope anomaly near Donghai in Jiangsu Province, China: Geochimica et Cosmochimica Acta, v. 66, p. 2299–2306.

Rumble, D., Liou, J. G., and Jahn, B.-m., 2003, Continental crust subduction and ultrahigh pressure metamorphism: Treatise on Geochemistry, v. 3, p. 293–319.

Rumble, D. and Yui, T.-F., 1998, The Qinglongshan oxygen and hydrogen isotope anomaly near Donghai in Jiangsu province, China: Geochimica et Cosmochimica Acta, v. 62, p. 3307–3321.

Shaffer, E. W., Sang, S-L. J., Cooper, A. R., and Heuer, A. H., 1974, Diffusion of tritiated water in ß-quartz, *in* Hofmann, A. W., Giletti, B. J., Yoder, H. S., Jr., and Yund, R. A., eds., Geochemical kinetics and transport: Carnegie Institute of Washington Publication, v. 634, p. 131–138.

Sharp, Z. D, O'Neil, J. R., and Essene, E. J., 1988, Oxygen isotope variations in granulite-grade iron formation: Constraints on oxygen diffusion and retrograde isotopic exchange: Contributions to Mineralogy and Petrology, v. 98, p. 490–501.

Sharp, Z. D., Atudorei, V., and Durakiewicz, T., 2001, A rapid method for determination of hydrogen and oxygen isotope ratios from water and hydrous minerals: Chemical Geology, v. 178, p. 197–210.

Smyth, J. R., Bell, D. R., and Rossman, G. R., 1991, Incorporation of hydroxyl in upper mantle clinopyroxenes: Nature, v. 351, p. 732–734.

Stalder, R., and Skogby, H., 2003, Hydrogen diffusion in natural and synthetic orthopyroxene: Physics and Chemistry of Minerals, v. 30, p. 12–19.

Su, W., You, Z.-D., and Cong, B.-L., 2002, Cluster of water molecules in garnet from ultrahigh-pressure eclogite: Geology, v. 30, p. 611–614.

Suzuoki, T., and Epstein, S., 1976, Hydrogen isotope fractionation between OH-bearing minerals and water: Geochimica et Cosmochimica Acta, v. 40, p. 1229–1240.

Thompson, A. B., 1992, Water in the Earth's upper mantle: Nature, v. 358, p. 295–302.

Valley, J. W., 2003, Oxygen isotopes in zircon, *in* Hanchar, J. M., and Hoskin, P. W. O., eds., Zircon: Washington, DC, Mineralogical Society of America, Reviews in Mineralogy and Geochemistry, v. 53, p. 343–385.

Valley, J. W., Kinny, P. D., Schulze, D. J., Spicuzza, M. J., 1998, Zircon megacrysts from kimberlite: Oxygen isotope variability among mantle melts: Contributions to Mineralogy and Petrology, v. 133, p. 1–11.

Valley, J. W., Kitchen, N., Kohn, M. J., Niendorf, C. R., and Spicuzza, M. J., 1995, UWG-2, a garnet standard for oxygen isotope ratio: Strategies for high precision and accuracy with laser heating: Geochimica et Cosmochimica Acta, v. 59, p. 5223–5231.

Wan, Y., Li, R. W., Wilde, S. A., Liu, D. Y., Chen, Z. Y., Yan, L. L., Song, T. R., and Yin, X. Y., 2005, UHP metamorphism and exhumation of the Dabie Orogen, China: Evidence from SHRIMP dating of zircon and monazite from a UHP granitic gneiss cobble from the Hefei Basin: Geochimica et Cosmochimica Acta, v. 69, p. 4333–4348.

Wang, L. P., Zhang, Y. X., and Essene, E. J., 1996, Diffusion of the hydrous in pyrope: American Mineralogist, v. 81, p. 706–718.

Wang, X., Liou, J. G., and Mao, H. K., 1989, Coesite-bearing eclogite from Dabie Mountains in Central China: Geology, v. 17, p. 1085–1088.

Wang, Y. X., Yang, J. D., Tao, X. C., and Li, H. M., 1988, A study of the Sm-Nd method for fossil, mineral, rock and its application: Journal of Nanjing University (Natural Science Edition), v. 24(2), p. 297–308 (in Chinese with English abstract).

Wiedenbeck, M., Alle, P., Corfu, F., Griffin, W. L., Meier, M., Oberli, F., von Quadt, A., Roddick, J. C., and Spiegel, W., 1995, Three natural zircon standards for U-Th-Pb, Lu-Hf, trace element, and REE analyses: Geostandard Newsletter, v. 19, p. 1–23.

Withers, A. C., Wood, B. J., and Carroll, M. R., 1998, The OH content of pyrope at high pressure: Chemical Geology, v. 147, p. 161–171.

Woods, S. C., Mackwell, S., and Dyar, D., 2000, Hydrogen in diopside: Diffusion profiles: American Mineralogist, v. 85, p. 480–487.

Xia, Q.-K., Sheng, Y.-M., Yang, X.-Z., and Yu, H.-M., 2005, Heterogeneity of water in garnets from UHP eclogites, eastern Dabieshan, China: Chemical Geology, v. 224, p. 237–246.

Xie, Z., Zheng, Y.-F., John, B.-m., Ballevre, M., Chen, J.-F., Gautier, B., Gao, T.-S., Gong, B., and Zhou, J.-B., 2004, Sm-Nd and Rb-Sr dating of pyroxene-garnetite from North Dabie in east-central China: Problem of isotope disequilibrium due to retrograde metamorphism: Chemical Geology, v. 206, p. 137–158.

Xu, S., Okay, A. I., Ji, S., Sengor, A. M. C., Su, W., Liu, Y., and Jiang, L., 1992, Diamond from Dabie Shan metamorphic rocks and its implication for tectonic setting: Science, v. 256, p. 80–82.

Yao, Y., Ye, K., and Liu, J., 2000, A transitional eclogite- to high pressure granulite–facies overprint on coesite-eclogite at Taohang in the Sulu ultrahigh-pressure terrane, eastern China: Lithos, v. 52, p. 109–120.

Ye, K., Yao, Y., and Katayama, I., 2000, Large areal extent of ultrahigh-pressure metamorphism in the Sulu ultrahigh-pressure terrane of East China: New implications from coesite and omphacite inclusions in zircon of granitic gneiss: Lithos, v. 52, p. 157–164.

Yuan, H.-L., Gao, S., Liu, X.-M., Li, H.-M., Gunther, D., and Wu, F.-Y., 2004, Accurate U-Pb age and trace element determinations of zircon by laser ablation-inductively coupled plasma mass spectrometry: Geostandards and Geoanalytical Research, v. 28, p. 353–370.

Yui, T.-F., Rumble, D., Chen, C.-H., and Lo, C.-H., 1997, Stable isotope characteristics of eclogites from the ultra-high-pressure metamorphic terrain, east-central China: Chemical Geology, v. 137, p. 135–147.

Yui, T.-F., Rumble, D., and Lo, C.-H., 1995, Unusually low $\delta^{18}O$ ultra-high-pressure metamorphic rocks from the Sulu Terrane, eastern China: Geochimica et Cosmochimica Acta, v. 59, p. 2859–2864.

Zhang, J. F., Jin, Z. M., Green, H. W., and Jin, S. Y., 2001, Hydroxyl in continental deep subduction zone: Evidence from UHP eclogites of the Dabie Mountains: Chinese Science Bulletin, v. 46, p. 592–595.

Zhang, J. F., Green, H. W., Bozhilov, K., and Jin, Z. M., 2004, Faulting induced by precipitation of water at grain boundaries in hot subducting oceanic crust: Nature, v. 428, p. 633–636.

Zheng, Y.-F., 1991, Calculation of oxygen isotope fractionation in metal oxides: Geochimica et Cosmochimica Acta, v. 55, p. 2299–2307.

Zheng, Y.-F., 1993a, Calculation of oxygen isotope fractionation in anhydrous silicate minerals: Geochimica et Cosmochimica Acta, v. 57, p. 1079–1091.

Zheng, Y.-F., 1993b, Calculation of oxygen isotope fractionation in hydroxyl-bearing silicates: Earth and Planetary Science Letters, v. 120. p. 247–263.

Zheng, Y.-F. and Fu, B., 1998, Estimation of oxygen diffusivity from anion porosity in minerals: Geochemical Journal, v. 32, p. 71–89.

Zheng, Y.-F., Fu, B., Gong, B., and Li, L., 2003a, Stable isotope geochemistry of ultrahigh pressure metamorphic rocks from the Dabie-Sulu orogen in China: Implications for geodynamics and fluid regime: Earth Science Reviews, v. 62, p. 105–161.

Zheng, Y.-F., Fu, B., Gong, B., and Li, S., 1996, Extreme ^{18}O depletion in eclogite from the Su-Lu terrane in East China: European Journal of Mineralogy, v. 8, p. 317–323.

Zheng, Y.-F., Fu, B., Li, Y.-L., Wei, C.-S., and Zhou, J.-B., 2001, Oxygen isotope composition of granulites from Dabieshan in eastern China and its implications of for geodynamics of Yangtze plate subduction: Physics and Chemistry of Earth (A), v. 26, p. 673–684.

Zheng, Y.-F., Fu, B., Li, Y.-L., Xiao, Y.-L., and Li, S.-G., 1998, Oxygen and hydrogen isotope geochemistry of ultrahigh-pressure eclogites from the Dabie Mountains and Sulu terrane: Earth and Planetary Science Letters, v. 155, p. 113–129.

Zheng, Y.-F., Fu, B., Xiao, Y.-L, Li, Y.-L., and Gong, B., 1999, Hydrogen and oxygen isotope evidence for fluid-rock interactions in the stages of pre- and post- UHP metamorphism in the Dabie Mountains: Lithos, v. 46, p. 677–693.

Zheng, Y.-F., Wang, Z.-R., Li, S.-G., and Zhao, Z.-F., 2002, Oxygen isotope equilibrium between eclogite minerals and its constraints on mineral Sm-Nd chronometer: Geochimica et Cosmochimica Acta, v. 66, p. 625–634.

Zheng, Y.-F., Wu, Y.-B., Chen, F.-K., Gong, B., Li, L., and Zhao, Z.-F., 2004, Zircon U-Pb and oxygen isotope evidence for a large-scale ^{18}O depletion event in igneous rocks during the Neoproterozoic: Geochimica et Cosmochimica Acta, v. 68, p. 4145–4165.

Zheng, Y.-F., Wu, Y.-B., Zhao, Z.-F., Zhang, S.-B., Xu, P., and Wu, F.-Y., 2005a, Metamorphic effect on zircon Lu-Hf and U-Pb isotope systems in ultrahigh-pressure eclogite-facies metagranite and metabasite: Earth and Planetary Science Letters, v. 240, p. 378–400.

Zheng, Y.-F., Yang, J.-J., Gong, B., and Jahn, B.-m., 2003b, Partial equilibrium of radiogenic and stable isotope systems in garnet peridotite during UHP metamorphism: American Mineralogist, v. 88, p. 1633–1643.

Zheng, Y.-F., Zhao, Z.-F., Li, S.-G., and Gong, B., 2003c, Oxygen isotope equilibrium between ultrahigh-pressure metamorphic minerals and its constraints on Sm-Nd and Rb-Sr chronometers, *in* Vance, D., Muller, W., and Villa, I. M., eds., Geochronology: Linking the isotope record with petrology and textures: Geological Society Special Publication, v. 220, p. 93–117.

Zheng, Y.-F., Zhao, Z.-F., Wu, Y.-B., Zhang, S.-B., Liu, X. M., and Wu, F.-Y., 2006, Zircon U-Pb age, Hf and O isotope constraints on protolith origin of ultrahigh-pressure eclogite and gneiss in the Dabie orogen: Chemical Geology, v. 231, p. 135–158.

Zheng, Y.-F., Zhou, J.-B., Wu, Y.-B., and Xie, Z., 2005b, Low-grade metamorphic rocks in the Dabie-Sulu orogenic belt: A passive-margin accretionary wedge deformed during continent subduction: International Geology Review, v. 47, p. 851–871.